12-2023

Uncertainty Quantification Framework for Design Optimization

Austin Ryan Williams
awill271@vols.utk.edu

To the Graduate Council:

I am submitting herewith a thesis written by Austin Ryan Williams entitled "Uncertainty Quantification Framework for Design Optimization." I have examined the final electronic copy of this thesis for form and content and recommend that it be accepted in partial fulfillment of the requirements for the degree of Master of Science, with a major in Nuclear Engineering.

Sandra Bogetic, Major Professor

We have read this thesis and recommend its acceptance:

Jason Hayward, Vladimir Sobes

Accepted for the Council:
Dixie L. Thompson

Vice Provost and Dean of the Graduate School

(Original signatures are on file with official student records.)

To the Graduate Council:
I am submitting herewith a thesis written by Austin Williams entitled "Uncertainty Quantification Framework for Design Optimization." I have examined the final electronic copy of this thesis for form and content and recommend that it be accepted in partial fulfillment of the requirements for the degree of Master of Science, with a major in Nuclear Engineering.

Sandra Bogetic, Major Professor

We have read this thesis
and recommend its acceptance:

Vladimir Sobes

Jason Hayward

Accepted for the Council:

Carolyn R. Hodges

Vice Provost and Dean of the Graduate School

(Original signatures are on file with official student records.)

Uncertainty Quantification Framework for Design Optimization

A Thesis Presented for the

Master of Science

Degree

The University of Tennessee, Knoxville

Austin Williams

December 2023

I would like to dedicate this work to all those who have helped me through my academic career. Thank you so much LeAnna, Mom, Dad, Braden, Darci, and Reba.

Acknowledgements

I would like to thank my academic advisor Dr. Sandra Bogetic, my mentor Dr. Jeffrey Favorite, and my research group for all the help with this work. This material is based upon work supported by the Department of Energy National Nuclear Security Administration through the Nuclear Science and Security Consortium under Award Number(s) DE-NA0003996.

Abstract

Difficulty to obtain neutron sources of interest have driven the need for optimization techniques to tailor a neutron generator as a replacement. A proposed solution uses off-the-shelf neutron sources coupled with an energy-tuning assembly to mimic the source of interest (i.e. AmLi, AmBe, thermonuclear fission spectra, etc.). These energy-tuning assemblies have been designed with complex optimization algorithms coupled with Monte Carlo simulations. These new system surrogate designs often do not have an experimental counterpart for validation and comparison, and lack non-statistical uncertainties. This work aims to improve confidence in the predictions by providing a tool for fast uncertainty quantification to use with transport tools, necessary for future validations. The tool, TOFFEE, has been developed to use the sensitivity coefficients and covariance data along with the sandwich rule to assign variance in cross-section data and subsequentially to reaction rates, neutron flux, and k-eff.

TOFFEE is a Python framework that uses MCNP6.3 to calculate sensitivity coefficients (generated by KSEN, PERT, etc.) and NJOY to generate a covariance library. The tool generates new input files and calculates the cross-section uncertainty with the sandwich rule. To test the tool, TOFFEE is used to generate cross-section uncertainty on three models: two benchmarks, Jezebel, BeRP ball, and a newly generated energy-tuning assembly designed with an advanced optimization algorithm. The results presented in the example application are the uncertainty on k_{eff} for Jezebel, the uncertainty on k_{eff} and the volumetric flux for the BeRP ball. The

examples are then verified by comparing them to the stochastic sampling method for calculating uncertainty, used in the SAMPLER routine by SCALE. Lastly, the uncertainty in the energy-dependent surface flux leaving the energy-tuning assembly is calculated. These three examples give confidence that the tool can be used standalone and in the optimization process of energy-tuning assemblies for source replacement.

Table of Contents

List of Tables

List of Figures

Nomenclature

ϕ	Scalar Flux
ψ	Angular Flux
Σ	Macroscopic Cross-section
σ	Microscopic Cross-section
k_{eff}	Effective Multiplication Factor
S	Relative Sensitivity Coefficient

Chapter 1

Introduction

The scientific community has had a strong interest in understanding and capability to model how neutrons travel through matter since the discovery of the neutron Wigner and Breit (1992); De Gregorio (2005); Variansyah et al. (2023) and such effort led to the discovery of fission in 1938 Hahn and Strassmann (1938). The discovery of fission and the beginnings of World War II motivated the work on fission weapons. During the construction of the atomic weapons, a strong theoretical understanding of nuclear physics has been developed. For example, the United States Manhattan Project devised much of the theory we still use for neutron physics.

Today, many complex nuclear problems are solved with neutron transport, i.e. reactor simulation Shaw et al. (2023), criticality safety Depriest et al. (2022), safeguards Rising and Bolding (2022), and experiment design Conant et al. (2023). One of the most popular methods to solve these problems uses the statistical Monte Carlo (MC) method to simulate the reality of the neutron events. Nevertheless, Monte Carlo simulation presents uncertainties that need to be quantified to better understand predictions of a design. A prominent uncertainty of the Monte Carlo Method is the uncertainty of the probability distribution functions within the nuclear data, which are used to solve the transport problem.

Accounting for such uncertainties is of large importance in the prediction of new nuclear systems that have not been deployed. Being able to quantify uncertainties in the system is helpful for designers to understand the predicted results and improve the optimization of the design. Subsection 1.1 discusses examples of new systems that have been designed using complex optimization methods and could benefit from uncertainty quantification within the design process.

1.1 Complex Optimized Designs

Some neutron sources are becoming scarce or expensive to acquire Winch et al. (2017); Yinghuai and Hosmane (2013). No nuclear weapons are tested and fewer nuclear reactors are being built. Thus, a need has arisen to design alternative sources that mimic advanced reactors, isotopic sources, nuclear explosions, etc. Common recent method have been developed, as alternative source, that used neutron generators together with optimized energy-tuning assemblies (ETA).

An example is Athena, which is an ETA that is designed to shape the deuterium-tritium (D-T) source at the National Ignition Facility (NIF) to mimic a thermonuclear plus prompt fission neutron spectrum Quartemont et al. (2021). Figure 1.1 shows a 3-D model of Athena. This spectrum is important for testing radiation effects on materials and components. It is designed using the metaheuristics algorithm Gnowee Bevins and Slaybaugh (2019); Bogetic et al. (2018) coupled with a MC transport code. The key characteristic of this model is the shape of the neutron spectrum in energy. For this model, the uncertainty in the neutron spectrum was calculated after the optimization process.

Neutron sources from (alpha,n) reactions have been frequently used for nuclear security applications, i.e. AmLi for active well coincidence counting McElroy and Cleveland (2017, 2018); Williams and Bogetic (2020). Recently, access to those isotopes has been limited, therefore there is a need to replace these sources with an easy-to-access generator(D-D and D-T) coupled with an ETA to tailor the spectra

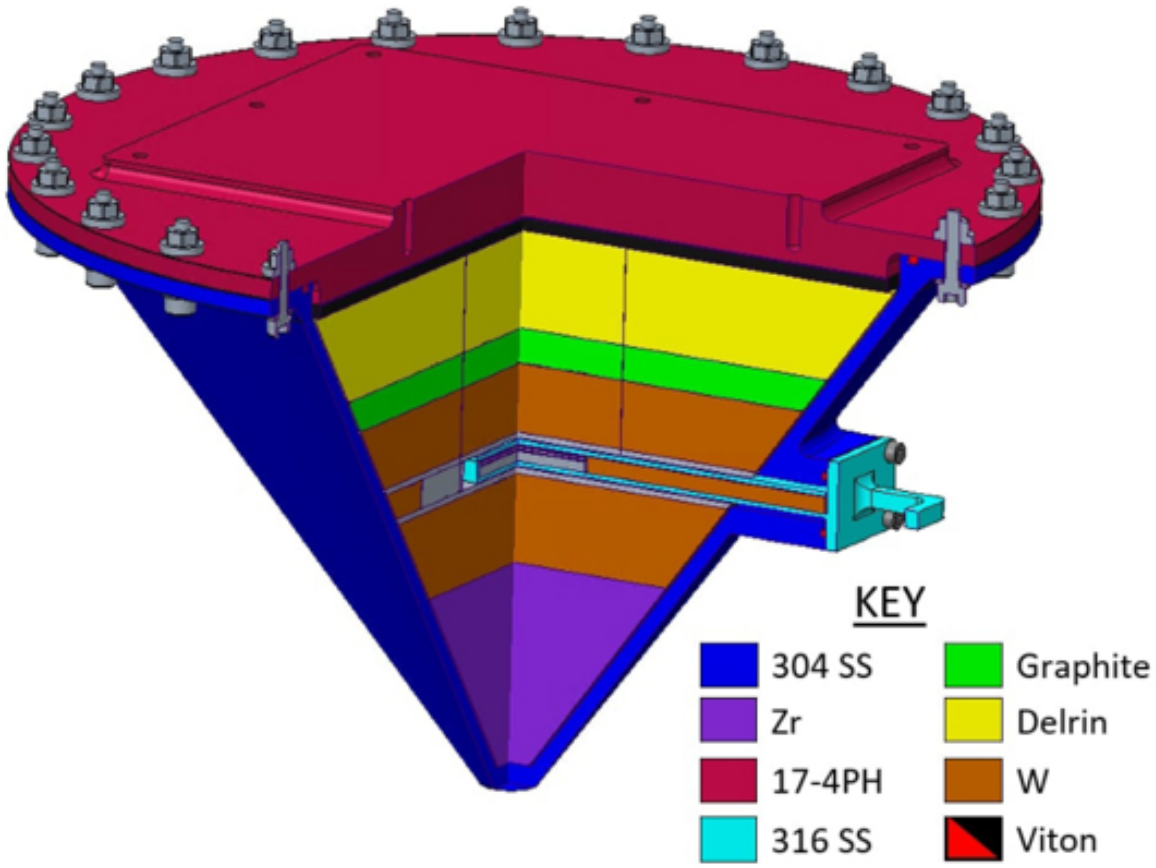

Figure 1.1: This figure shows a 3-D visualization of the Athena energy-tuning assembly Quartemont et al. (2021)

to lower neutron energies. Designing an ETA requires complex optimization due to multiple variables and constraints that affect the path and energy of the neutrons. Thus, the advantage of using codes like Gnowee coupled with MC is that they are able to design an ETA optimized with a D-D neutron source to replace an AmLi source for maximizing fissions of isotopes of interest (i.e. U-235).

Another example of a surrogate neutron source is the Fast Neutron Source (FNS) at the University of Tennessee, Knoxville. The FNS is designed as a subcritical multiplication experiment that replicates the neutron spectra of fast reactors. The FNS is designed as an integral experiment facility to help improve cross-section data availability and support advanced reactors Hines et al. (2018); Sobes et al. (2022); Pevey et al. (2020, 2022). Figure 1.2 shows a theoretical model of the FNS. Methods have been explored to design the FNS using a genetic algorithm and the MC code, MCNP6.2.

All the above designs have been performed using state-of-the-art MC codes in the nuclear community, that provide only statistical uncertainties to the simulation results. Thus, no cross-section uncertainty analysis is considered in the process of these designs. Most of the ETA include one or more filter or multiplying materials, and the lack of cross-sectional uncertainties on the reactions for all the material limits the fidelity of the alternative sources. Thus, it is important to perform simulations and optimization with correctly propagated uncertainties of the data of the materials used in the design of the ETA and complex nuclear systems.

1.2 Research Objective

This work aims to fill the need for a cross-section uncertainty analysis by developing a framework, TOFFEE, that calculates uncertainties for reaction rate, flux, and k_{eff} from cross-section propagation. This is needed in the design process and is subsequently suited for the optimization of nuclear systems.

The goal of the framework is to provide an uncertainty on the quantity of interest for many types of systems that could be optimized, from the sensitivities provided by the users or routines such as the general perturbation theory of MCNP, Scale, Serpent, etc. This framework also needs to be fast in order to calculate the uncertainty alongside each potential model.

1.3 Thesis Outline

The work is organized in 5 chapters. Chapter 2 provides a background theory required in the development of the uncertainty framework, TOFFEE. Chapter 3 discusses the methodology applied to develop and use the framework. Next, the framework will be used for several applications, i.e. benchmarks and new designs, and those applications are reported in Chapter 4. Then, the conclusions and future work of the analysis will be discussed in Chapter 5.

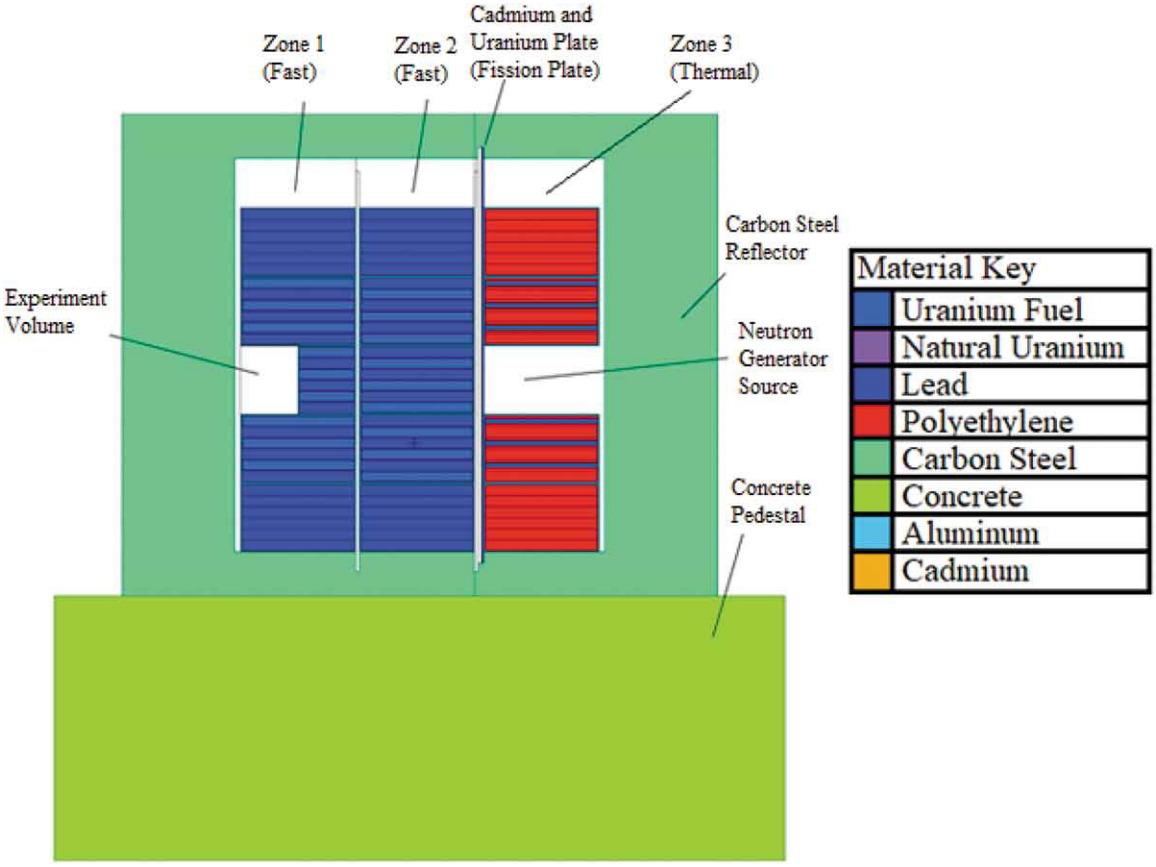

Figure 1.2: This figure shows a visualization of the potential design for the Fast Neutron Source at the University of Tennessee, Knoxville Pevey et al. (2020)

Chapter 2

Background

This chapter discusses the background required to understand the fundamentals of this thesis work. A description of the Boltzmann equation and how it applies to neutron transport is initially given. Next, this work discusses the nuclear data that is used in the application. The process of quantifying uncertainty is then discussed as they are applied in this work. Then, the Monte Carlo method is described as it is used for neutron transport. Finally, the concept of a benchmark experiment is discussed first.

2.1 Transport Theory

The study of how a particle moves through matter is typically referred to as transport theory Davison (1957). Transport theory is used to track the location, direction, energy, and time of a particle as it moves and interacts within a medium. This can be used to give important system information such as the effective multiplication factor (k_{eff}), neutron flux(ϕ), or fission rate. These characteristics are used to determine if a nuclear system is performing as it was designed to perform. Today, transport theory is used for many nuclear applications including reactor theory, criticality safety, nonproliferation, and stockpile stewardship.

2.1.1 Boltzmann Equation

The equation that governs the transport of neutrons through a medium is the Boltzmann equation Lewis and Miller (1984). This equation was originally used for the transport of gas particles in a thermodynamic system. The use of the Boltzmann equation for neutron transport can be seen before the beginning of the Manhattan Project.

Before the discussion of the different forms of the Boltzmann equation, the key components of the equation must first be defined. The particle density at location $\vec{r}$, traveling in the direction $\hat{\Omega}$, at energy E, at time t is defined as $N(\vec{r}, \hat{\Omega}, E, t)dVd\hat{\Omega}dEdt$. Therefore, $N(\vec{r}, \hat{\Omega}, E, t)$ can be thought of as the number of particles per unit volume, solid angle, energy, and time. Angular flux, denoted $\psi(\vec{r}, \hat{\Omega}, E, t)$, is defined as the distance traveled in the direction $\hat{\Omega}$, at location $\vec{r}$, at energy E, at time t. Equation 2.1 shows the relationship between angular flux and particle density where v is the velocity of the particle.

$$\psi(\vec{r}, \hat{\Omega}, E, t) = vN(\vec{r}, \hat{\Omega}, E, t) \tag{2.1}$$

The scalar flux, denoted $\phi(\vec{r}, E, t)$, is the angular integrated angular flux as shown in equation 2.2.

$$\phi(\vec{r}, E, t) = \int \psi(\vec{r}, \hat{\Omega}, E, t)d\hat{\Omega} \tag{2.2}$$

The number of x (i.e fission, capture, etc) reactions as a function of location and time, denoted $R_x(\vec{r}, t)$, can be calculated using equation 2.3.

$$R_x(\vec{r}, t) = \int \Sigma_x(\vec{r}, E)\phi(\vec{r}, E, t)dE \tag{2.3}$$

The general form of the Boltzmann equation with time, spacial, energy, and angular dependence is shown in equation 2.4 for Cartesian coordinates, where Σ_t

is the total macroscopic cross-section and q is the production of particles within the system.

$$\frac{1}{v}\frac{\partial\psi}{\partial t} + \hat{\Omega}\cdot\vec{\nabla}\psi(\vec{r},\hat{\Omega},E,t) + \Sigma_t(\vec{r},E,t)\psi(\vec{r},\hat{\Omega},E,t) = q(\vec{r},\hat{\Omega},E,t) \tag{2.4}$$

In the Boltzmann equation, the term $\frac{1}{v}\frac{\partial\psi}{\partial t}$ represents the total change in particle population with respect to time, such as particle decay. The term $\hat{\Omega}\cdot\vec{\nabla}\psi(\vec{r},\hat{\Omega},E,t)$ represents net streaming of particles out of the system. The term $\Sigma_t(\vec{r},E,t)\psi(\vec{r},\hat{\Omega},E,t)$ represents the particles lost to collisions (reactions).

2.1.2 Source-Driven Boltzmann Equation

Equation 2.4 is a general form for any particle transport. The q term must be better defined in order to form an equation that is specific to neutron transport. There are three primary methods by which neutrons can be gained: an external neutron source, reaction production, and neutron scattering.

An external neutron source, denoted $q_{external}(\vec{r},\hat{\Omega},E,t)$, is defined as some determined amount of neutrons that are to be injected into the system with some given parameters. This is the source of the initial population of neutrons but does not necessarily only include source neutrons. A real-world example of this could be a Californium-252 neutron source or a Deuterium-Deuterium neutron generator.

Reaction production refers to the production of neutrons through a reaction that occurs within the system. The most common example of this is fission occurring within fissile material. When fission occurs, a number of neutrons are released into the system as part of the process. The fission production ($q_{fission}$) is defined in equation 2.5, where ν is the number of neutrons released from fission, Σ_f is the macroscopic fission cross-section, ω is a probability distribution that describes the angle of a neutron released from fission and χ is a probability distribution that describes the energy of a neutron released from fission.

$$q_{fission}(\vec{r},\hat{\Omega},E,t) = \omega(\hat{\Omega})\chi(\vec{r},E)\int \nu(\vec{r},E')\Sigma_f(\vec{r},E')\int \psi(\vec{r},\hat{\Omega}',E',t)d\hat{\Omega}'dE' \quad (2.5)$$

However, fission is not the only reaction that would fall into the category of reaction production. Another example is the (n,2n) reaction.

The last production term is neutron scattering ($q_{scattering}$). This might seem odd to call neutron scattering a "production" unless scattering is thought of as a neutron being absorbed at one energy and produced at another. Equation 2.6 shows how this can be applied to the production term, where Σ_s is the macroscopic scatter cross-section from energy E' direction $\hat{\Omega}'$ to energy E direction $\hat{\Omega}$.

$$q_{scatter}(\vec{r},\hat{\Omega},E,t) = \int\int \Sigma_s(\vec{r},\hat{\Omega}'\rightarrow\hat{\Omega},E'\rightarrow E)\psi(\vec{r},\hat{\Omega}',E',t)d\hat{\Omega}'dE' \quad (2.6)$$

After combining the three production terms, a simplification of a source-driven Boltzmann equation can be described as shown in equation 2.7.

$$\begin{aligned}\frac{1}{v}\frac{\partial\psi}{\partial t} + \hat{\Omega}\cdot\vec{\nabla}\psi(\vec{r},\hat{\Omega},E,t) + \Sigma_t(\vec{r},E,t)\psi(\vec{r},\hat{\Omega},E,t) &= q_{external}(\vec{r},\hat{\Omega},E,t) \\ &+ \int\int \Sigma_s(\vec{r},\hat{\Omega}'\rightarrow\hat{\Omega},E'\rightarrow E)\psi(\vec{r},\hat{\Omega}',E',t)d\hat{\Omega}'dE' \\ &+\omega(\hat{\Omega})\chi(\vec{r},E)\int \nu(\vec{r},E')\Sigma_f(\vec{r},E')\int \psi(\vec{r},\hat{\Omega}',E',t)d\hat{\Omega}'dE'\end{aligned} \quad (2.7)$$

2.1.3 k-Eigenvalue Boltzmann Equation

The source-driven form of the Boltzmann equation is only valid for systems where more neutrons are absorbed than produced. This is typically referred to as a subcritical system. In order to solve the Boltzmann equation for systems that are not subcritical, an adjustment factor is added to reduce the production of neutrons in the system. This factor is called the k-eigenvalue (or k-effective). The typical method to

use the k-eigenvalue is to apply it to ν in a steady-state (no external source) problem as shown in equation 2.8, where k is the largest k-eigenvalue.

$$\begin{aligned} \frac{1}{v}\frac{\partial\psi}{\partial t} + \hat{\Omega}\cdot\vec{\nabla}\psi(\vec{r},\hat{\Omega},E,t) + \Sigma_t(\vec{r},E,t)\psi(\vec{r},\hat{\Omega},E,t) = \\ \int\int \Sigma_s(\vec{r},\hat{\Omega}'\to\hat{\Omega},E'\to E)\psi(\vec{r},\hat{\Omega}',E',t)d\hat{\Omega}'dE' \\ +\omega(\hat{\Omega})\chi(\vec{r},E)\int\frac{\nu}{k}(\vec{r},E')\Sigma_f(\vec{r},E')\int\psi(\vec{r},\hat{\Omega}',E',t)d\hat{\Omega}'dE' \end{aligned} \tag{2.8}$$

2.1.4 Perturbation Theory

Perturbation theory refers to making a change to a system characteristic and observing the effects on other characteristics. An example of this for the k-eigenvalue Boltzmann equation is making a small change in the fission cross-section and determining the perturbed k-eigenvalue. This can be used to calculate the absolute sensitivity coefficient (approximation of the derivative) as shown in equation 2.9, where k_p is the perturbed k-eigenvalue, k_0 is the original k-eigenvalue, Σ_f' is the perturbed cross-section, and Σ_f is the original cross-section.

$$\frac{dk}{d\Sigma_r} = \frac{k_p - k_0}{\Sigma_r' - \Sigma_r} \tag{2.9}$$

2.2 Nuclear Data

Nuclear data refers to the data that quantifies how a particle interacts with matter. A commonly known example of nuclear data is the decay constant, which quantifies how frequently a nuclide emits radiation. For this work, the most commonly used nuclear data is the neutron cross-section.

2.2.1 Neutron Cross-Section Data

The neutron cross-section is a way the nuclear data evaluator can quantify the probability of a nuclear interaction occurring. The cross-section describes the number

of reactions that occur from a particle traveling across some surface area with respect to particle flux. A cross-section is given for a specific reaction, such as fission which is typically denoted as (n, fission), for a nuclide (such as Uranium-235) in which the reaction can occur. An example of a cross-section can be seen in Figure 2.1. These data are given (with respect to incoming particle energy) by an evaluation group such as ENDF Brown et al. (2018), JEFF Plompen et al. (2020), etc. Cross-section data is the primary data component of neutron transport.

2.2.2 Uncertainty in Nuclear Data

The uncertainty given to a cross-section describes the impact of the uncertainty in the available set of experimental data. This uncertainty is given in a covariance matrix with respect to energy. A covariance matrix is a mathematical way of showing the correlation of the uncertainty of a function for a given vector. The diagonal of the covariance matrix represents the variance of the function with respect to the vector. For nuclear cross-sections, the vector is given in a group-based energy structure. The general form of the energy vector can be seen in equation 2.10.

$$\vec{E} = [E_{n+1}, E_n, ...E_1, E_0], E_{n+1} < E_n < ... < E_1 < E_0 \tag{2.10}$$

For this case, the energy group structure has a length of $n + 1$, and the covariance matrix is a $n \times n$ matrix. The (0,0) element of the covariance matrix represents the variance of the cross-section between energies E_1 and E_0. The diagonal of the matrix represents the variance of the cross-section with respect to the energy groups. The off-diagonal components of the cross-section covariance matrix describe the effect of the uncertainty of one group on another.

Cross-section data has two limitations at the moment. The first issue is some key cross-sections having large uncertainties, especially at higher energies. An example can be seen in Figure 2.2 where the uncertainty is greater than 20 % percent for high energy neutrons. The second limitation is the lack of available data. Some

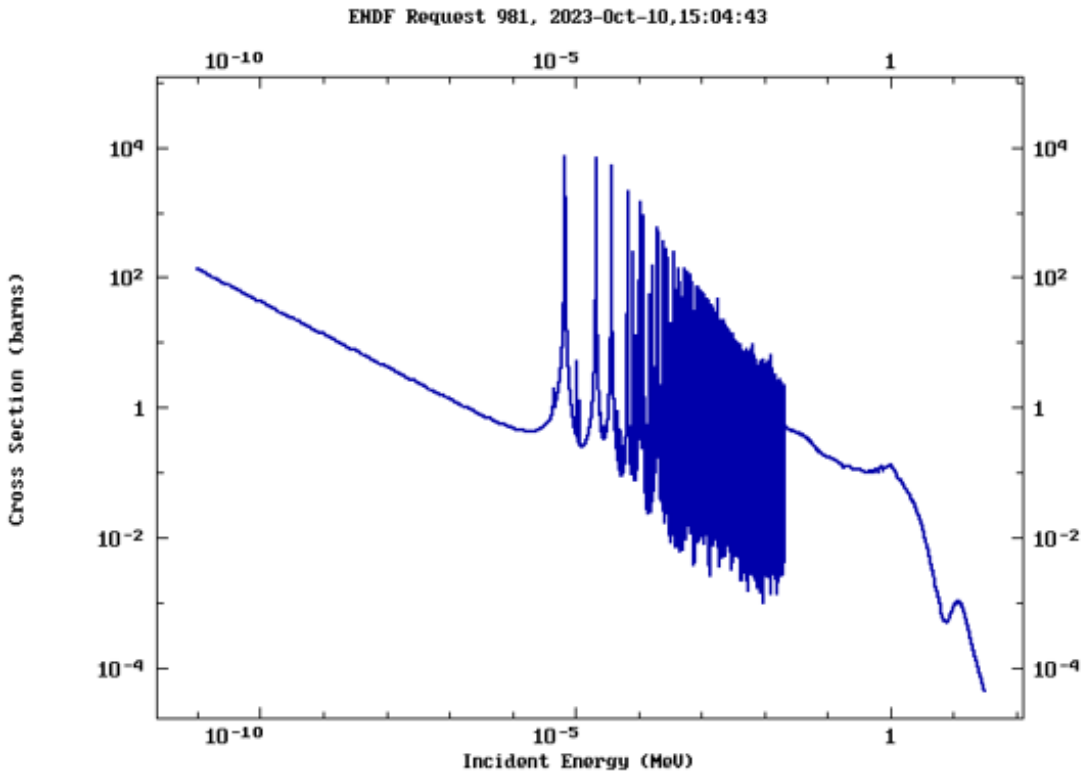

Figure 2.1: This figure shows the (n,γ) cross-section for Uranium-235.

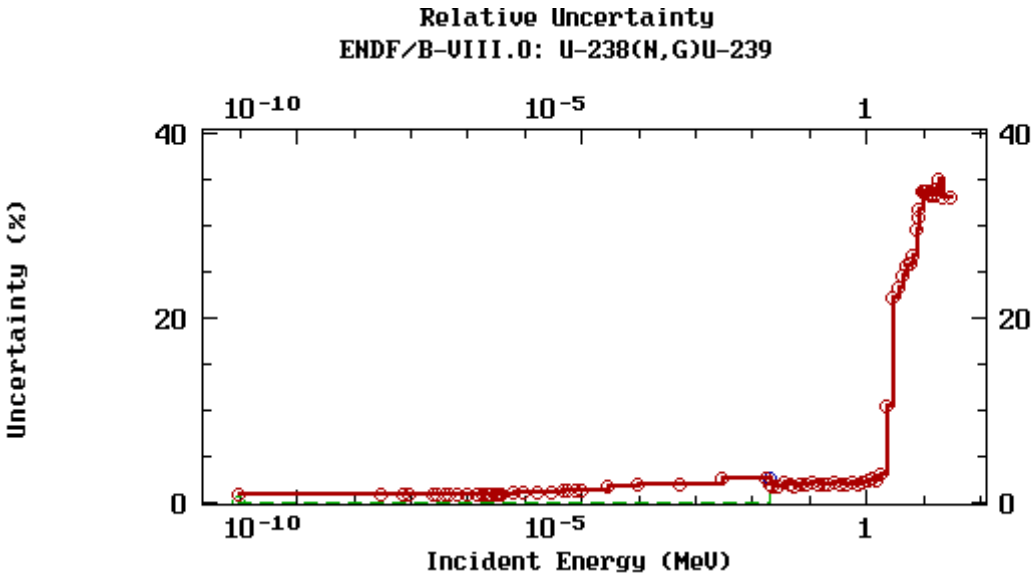

Figure 2.2: This figure shows the percent uncertainty in the (n,γ) cross-section for Uranium-235.

nuclides that were not present in the past experiments do not have experimental data to support an uncertainty prediction. This means that the cross-section given by the evaluators has no associated uncertainty even though the cross-section does have uncertainty in reality. However, some work has been done to improve the availability such as the BLO project Little et al. (2008) and the CIELO program Fleming et al. (2020).

2.3 Uncertainty Quantification

Uncertainty quantification is the act of quantifying the effects of uncertainty in a parameter on a quantity of interest. This can help better understand why the prediction technique (such as the Boltzmann equation) deviates from experimental results. This is useful for understanding the key contributors to uncertainty because it can inform future experimental needs.

2.3.1 Sensitivity Vector

A sensitivity vector refers to a vector of energy-dependent sensitivity coefficients as described in section 2.1.4. In this work, a sensitivity vector is structured such that it is a vector that represents the structure of the cross-section covariance data. This means that the sensitivity coefficients are calculated using equation 2.9 for changes in the cross-section for a single energy group. The sensitivity coefficients are calculated for each group. These coefficients S_i, as shown in equation 2.11 for the energy structure in equation 2.10, are used to form sensitivity vector $\vec{S}$.

$$\vec{S} = [S_0, S_1, ..., S_i, ..., S_{n-1}, S_n] \tag{2.11}$$

2.3.2 Sandwich Rule

The sandwich rule is a mathematical formula that allows the use of the covariance matrix and sensitivity vector to calculate variance for a function Kiedrowski et al. (2015). In the case of this work, the covariance matrix, $\mathbf{C}$ is structured as shown in equation 2.12, where $COV_{i,j}$ refers to the covariance value for energy group i with respect to energy group j.

$$\mathbf{C} = \begin{bmatrix} COV_{0,0} & COV_{0,1} & \cdots & COV_{0,n} \\ COV_{1,0} & COV_{1,1} & \cdots & COV_{1,n} \\ \vdots & \vdots & \ddots & \vdots \\ COV_{n,0} & COV_{n,1} & \cdots & COV_{n,n} \end{bmatrix} \tag{2.12}$$

Equation 2.13 shows the sandwich rule applied using this covariance matrix and the sensitivity vector from equation 2.11, where δ^2 is variance.

$$\delta^2 = \vec{S}\mathbf{C}\vec{S}^T \tag{2.13}$$

The sandwich rule for neutron transport with n cross-sections can be seen in equation 2.14 where $\vec{S}_i$ represents a sensitivity vector for cross-section i and $\mathbf{C}_{i,i}$ represents a covariance matrix for cross-section i with itself. The $\mathbf{C}_{i,0}$ is the covariance matrix between cross-section i and cross-section 0 and is the transpose of $\mathbf{C}_{0,i}$.

$$\delta^2 = \begin{bmatrix} \vec{S}_0 & \cdots \vec{S}_i \cdots \vec{S}_n \end{bmatrix} \begin{bmatrix} \mathbf{C}_{0,0} & \cdots & \mathbf{C}_{0,i} & \cdots & \mathbf{C}_{0,n} \\ \vdots & \ddots & & & \\ \mathbf{C}_{i,0} & \cdots & \mathbf{C}_{i,i} & \cdots & \mathbf{C}_{i,n} \\ \vdots & & & \ddots & \\ \mathbf{C}_{n,0} & \cdots & \mathbf{C}_{n,i} & \cdots & \mathbf{C}_{n,n} \end{bmatrix} \begin{bmatrix} \vec{S}_0 \\ \vdots \\ \vec{S}_i \\ \vdots \\ \vec{S}_n \end{bmatrix} \tag{2.14}$$

2.4 Monte Carlo Method for Neutron Transport

The Monte Carlo method is a stochastic approach to solving problems that are difficult (or impossible) to solve analytically. It has been applied to many fields such as financial engineering Glasserman (2004), mechanical engineering BUC and MASÁROVÁ (2013), and computer science Chowdhury et al. (2023). This method has been theorized and applied to neutron transport since the Manhattan Project Metropolis et al. (1958).

The basic approach to solving the transport equation using the Monte Carlo method is to sample the life of a neutron and keep track (tally) of the location and events the neutron experiences (reactions). The statistical average and standard deviation of the result are calculated based on the resulting tally with many neutron lives being simulated. Some of the key tallies that can be calculated include k_{eff}, flux, and reaction rate. One drawback to the Monte Carlo method for neutron transport is the need for computational power. Historically, Monte Carlo has struggled to model complicated systems due to limitations in computing power. With recent growth in computing power, the Monte Carlo method is able to solve problems such as a full-scale reactor Shaw et al. (2023).

2.5 Benchmark Experiments

A benchmark experiment is an experiment that is designed to mimic something that is difficult to create. An example of this is a nuclear weapon. Historically, nuclear material was very scarce, so models (such as Jezebel Favorite (2017b)) were created to run tests without using the material. Today, the US does not test nuclear weapons, but the characteristics of the materials are still desired to be understood. Benchmark experiments are a way to understand these characteristics. Historically, nuclear experiments have not been well documented, so previous data can be difficult to verify today. Today, a benchmark experiment requires a very detailed design so that

the experiment can be replicated in the future. The International Criticality Safety Benchmark Evaluation Project (ICSBEP) Agency (2023) has gathered a large number of benchmark experiments with restrictions on the completeness of documentation required for an experiment to be added to the book. A method to predict what is happening within these systems is needed to be able to extract the characteristics of the involved materials. Neutron transport theory can be used to examine how our theoretical ideas of these characteristics mimic reality.

Chapter 3

Modeling Methodology

This chapter describes the computational methods used to quantify the cross-sectional uncertainty for Monte Carlo evaluation. This research aims to develop a framework as a stand-alone capability that is compatible with multiple software that provide sensitivities. The primary goal of this work is a framework that supports MCNP simulations. The techniques for calculating sensitivity vectors using the methods available in MCNP-6.3 will be discussed first. Then, the method of extracting covariance data from neutron cross-section libraries using NJOY2016 will be described. Finally, the Python3 implementation to execute the matrix algebra and data analysis will be examined.

3.1 Neutronic Modeling

Today, the Monte Carlo method is one of the most popular methods of solving the Boltzmann equation for neutron transport. Monte Carlo N-Particle (MCNP) Kulesza et al. (2022) from Los Alamos National Lab is rooted in the origins of Monte Carlo but is still a state-of-the-art code today. SCALE Wieselquist and Lefebvre (2021) is a library of codes from Oak Ridge National Lab that includes several codes (MAVRIC, KENO, Shift, etc.) that implement the Monte Carlo method for neutron transport. OpenMC Romano et al. (2015) is an open-source Monte Carlo code that was written

by several graduate students for MIT. Serpent Leppänen et al. (2015) is another Monte Carlo code that is published by VVT in Finland. These are not all of the available codes but are very popular choices for most Monte Carlo neutron transport problems.

MCNP has roots in the first Monte Carlo programs for neutron transport Metropolis et al. (1958). Today, it is still at the forefront of transport solutions as a state-of-the-art Monte Carlo program. MCNP-6.3 is the latest version of MCNP which was released on August 29th, 2023. MCNP-6.3 was chosen due to its capability to produce k-eigenvalue and source-driven sensitivity coefficients.

MCNP-6.3 has two modes of execution this work will utilize: KCODE and SDEF. KCODE is used to solve the k-eigenvalue form of the Boltzmann equation described in section 2.1.3. SDEF is used to solve the source-driven Boltzmann equation as described in section 2.1.2.

3.1.1 k-Eigenvalue Sensitivity

The method to calculate the sensitivity coefficient of k_{eff} with respect to a cross-section is the MCNP method (referred to as card) KSEN Kiedrowski (2013). KSEN uses an advanced form of perturbation theory called Iterative Fission Probability to calculate the sensitivity coefficient. MCNP calculates the relative sensitivity coefficient. Equation 2.9 is the equation for absolute sensitivity. In order to get relative sensitivity, the equation must be normalized as shown in equation 3.1.

$$S_{r,k} = \frac{\Sigma_r}{k}\frac{dk}{d\Sigma_r} \tag{3.1}$$

In order to construct a sensitivity vector, KSEN must be given an energy structure. This structure will produce a list of sensitivity coefficients within the output file that can be used to construct a vector.

KSEN can also be given a set of cross-sections for desired sensitivity coefficients. These require the MT number for the cross-sections as described in MCNP documentation Kulesza et al. (2022). An example KSEN card is shown below for two energy groups, $(10^{-11}, 1)$ MeV and $(1, 20)$ MeV, and two cross-sections, MT = 2 (elastic scattering) and MT = 4 (inelastic scattering).

```
KSEN1 xs rxn = 2 4 erg = 1e-11 1.0 20.0
```

This command will report a sensitivity vector for all nuclides within the system for the described condition. For this reason, only one KSEN card is needed for the sensitivity vectors needed for this work. The energy discretization must match the structure of the covariance matrix data that is provided.

3.1.2 Source-Driven Sensitivity

The method to calculate a sensitivity vector for a source-driven sensitivity coefficient in MCNP uses the PERT card Favorite (2017a, 2021). Using the first and second-order differential technique, the PERT card gives the second-order Taylor's expansion. This work will look at only the first-order perturbations because only first-order sensitivity coefficients are used. If PERT is given the command "method=2", only the first-order difference of the tally value will be given. It should be noted that PERT uses density perturbations, not cross-section perturbations. This requires the use of atomic density as the perturbation due to its relationship with the macroscopic cross-section as shown in equation 3.2 where Σ is the macroscopic cross-section, ρ is atomic density, and σ is the microscopic cross-section.

$$\Sigma = \rho\sigma \tag{3.2}$$

Using this property, a PERT card can be used to get the perturbed tally, Δf, with respect to the initial tally, f for an atomic density perturbation factor a. The first-order relative sensitivity coefficient can be calculated as shown in equation 3.3.

$$S_{r,f} = \frac{\rho}{f}\frac{\Delta f}{a\rho} = \frac{\Sigma_r}{f}\frac{\Delta f}{a\Sigma_r} \tag{3.3}$$

This equation can be broken into energy discretization similar to k-eigenvalue sensitivities. This is done by having a unique PERT card for each energy group. PERT cards also require only one cross-section to change at a time. This requires a unique PERT card for each nuclide, reaction, and energy group present within the model. The two cards below are for a 2-group energy structure with a perturbation in the elastic scattering cross-section and one nuclide that is perturbed in material 2.

```
PERT1:n cell = 1 rho = 1.01 mat = 2 rxn = 2 method = 2 erg = 1e-11 1.0
PERT2:n cell = 1 rho = 1.01 mat = 2 rxn = 2 method = 2 erg = 1.0 20.0
```

3.1.3 Stochastic Sampling

The Sampler module in SCALE uses the stochastic sampling method to produce the cross-section uncertainty. This method uses the covariance data to randomly perturb the cross-sections within the nuclear data and reevaluates the problem with the updated data. This method is used in this work to compare with the sandwich rule method for calculating the uncertainty.

3.2 Nuclear Data Processing

The cross-section data given by the evaluator is given in different energy-group structures and at a different temperature than the problem. For these cases, a data processing code can be used to add factors, such as Doppler broadening, heating of the material, and resonance reconstruction. These codes can change the value of the data and change the structure of the data (energy groups). This can be useful for cross-sections and covariance matrices if a nonstandard case is used such as using a custom energy group structure. Two examples of these types of applications are

AMPX from SCALE Wiarda et al. (2015) and NJOY Kahler III and Macfarlane (2016) from Los Alamos National Laboratory (LANL).

NJOY Kahler III and Macfarlane (2016) is an open-source nuclear data evaluation code from Los Alamos National Laboratory. This work uses NJOY21 which is the most recent release of the program. NJOY allows for cross-section alterations such as resonance parameter reconstruction, Doppler broadening, and thermal scattering adjustments.

The modules used to construct the covariance matrix for this work can be seen in Figure 3.1. RECONR is the module to reconstruct the resonance parameters into the resonance cross-section in a point-wise ENDF format, PENDF. BROADR is the module that accounts for Doppler broadening in the PENDF cross-section. THERMR adds the thermal scattering point-wise data to the cross-section. The ERRORR module takes the original ENDF6 file and the generated PENDF file and creates a covariance matrix. ERRORR allows for user-defined energy-group structure to be given for the covariance matrix. The NJOY input file framework can be seen in Appendix A.1.

3.3 TOFFEE Framework

An open-source Python Framework is developed to combine these functions to calculate the variances for several parameters. The framework, TOol For Fast Error Estimation (TOFFEE), reads an MCNP input file to determine the nuclides and mode of the model. Next, a new MCNP input file is written alongside the necessary NJOY input files for the given nuclides. Then, these files are read and the sandwich rule is executed for all cross-sections. Finally, the variances are reported. Figure 3.1 shows a graphical representation of this Python Framework. This framework is available here:

https://github.com/NE-UTK-Computation-Lab/Cross-Section-Uncertainty

The framework includes a series of subroutines to manipulate software input files, run scripts on high-performance computers, perform matrix algebra, generate variances, and data plotting/imaging.

A Python script has been developed to allow for the reading of text from files with the use of the built-in open function. Python is a popular high-level programming language. It was chosen for this work because of its capabilities to read and write text files, interact with system-level functions, and construct useful data structures and plots. Python version 3.6.8 was used for this work.

A file manipulation capability is very useful for the framework application to automate read and write to input and output files from MCNP and NJOY, as well as, ENDF6 files. This is used to convert the text data from these files into useful information for the user.

The MCNP input file is used to determine the mode (KCODE or SDEF) the model will use, and the nuclides that are present in the materials. The required sensitivity cards are then added to the MCNP input file needed to calculate the sensitivity coefficients. The sensitivity coefficients are then read from the output file from the updated MCNP input file.

The material information is written to the NJOY input file to generate the covariance matrix. The covariance matrix is read from the output file from NJOY.

Both MCNP6.3 and NJOY are used on a remote computer that requires a batch script to execute. This requires the use of the Python module os to interact with the system command line using the os.system function.

The matrix operations used to execute the sandwich rule come from the Python module Numpy. These operations include transpose (numpy.transpose) and matrix multiplication (numpy.matmul). These operations allow the calculation of the variance for each sensitivity vector from MCNP and the covariance matrix from NJOY.

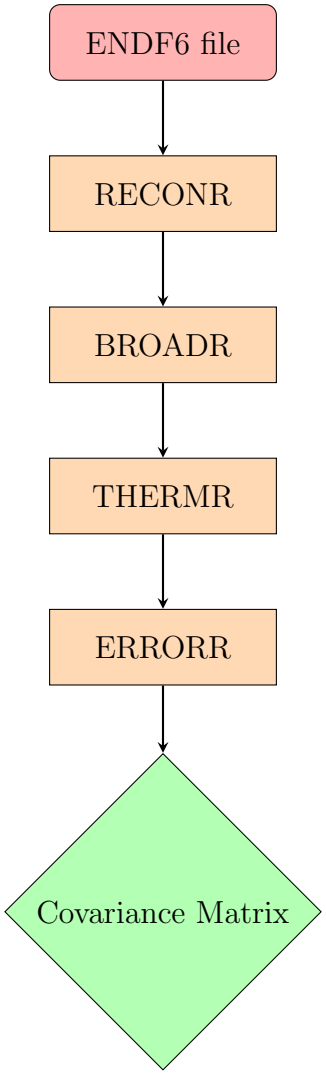

Figure 3.1: This is a graphical representation of the algorithm used with NJOY to produce a covariance matrix.

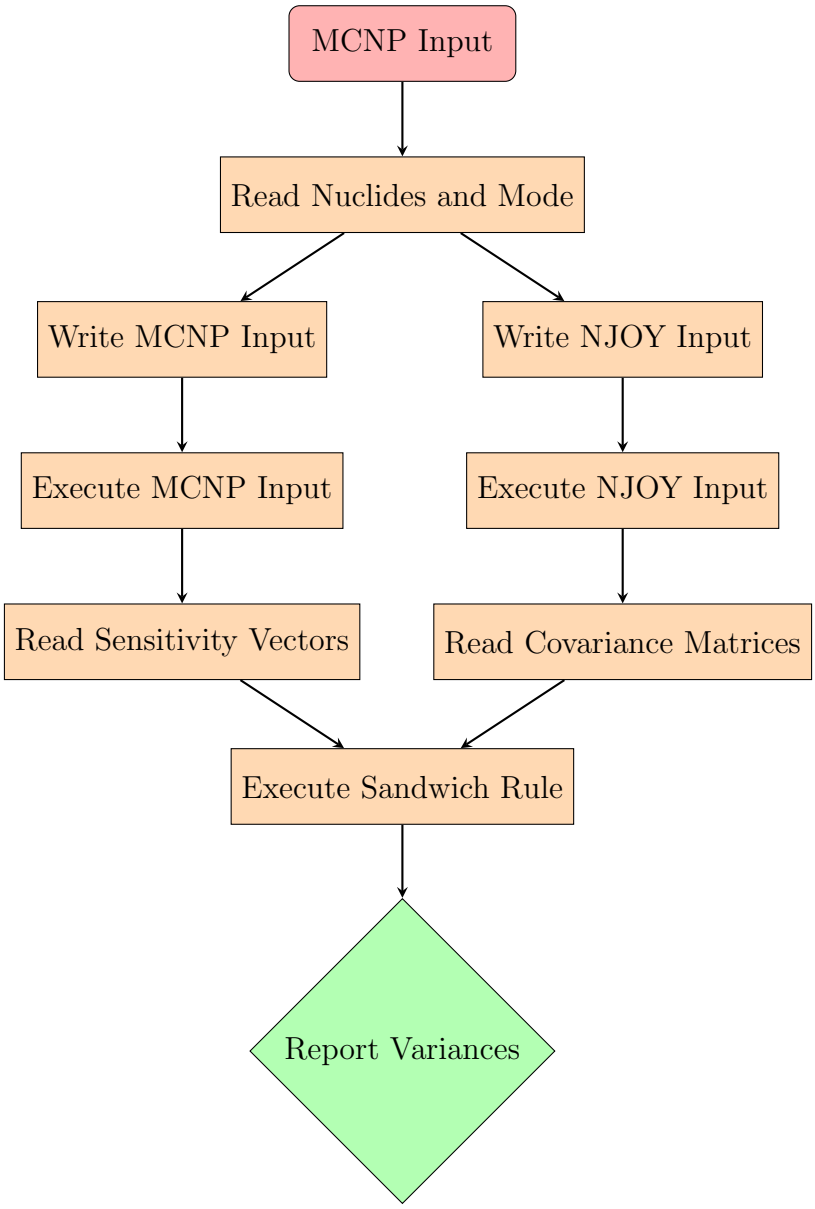

Figure 3.2: This is a graphical representation of the Python Framework used to calculate the variances using MCNP and NJOY.

Python has many tools that allow for data presentation. This work utilizes several of these tools to represent the data from the framework. The first is using the file editing methods to write a text file with the variances sorted from greatest to least. This is a simple representation that allows for the exact values to be easily extracted from a text file. A similar method used is the dictionary in Python. This is a Python structure that allows us to save all of the information within the Python data. This is only visible using commands or an IDE but is a very simple method of structuring the data. The framework uses the module pickle to save this for reference after the execution of the code.

Matplotlib is a Python module that generates plots. This module is used to generate a bar plot of the top five contributors to the variance. It is also used to generate plots of the sensitivity vectors for each nuclide and reaction. An example of this can be seen in Figure 3.3. Lastly, the covariance matrices are plotted as a heat map using the matshow function. An example of this can be seen in Figure 3.4.

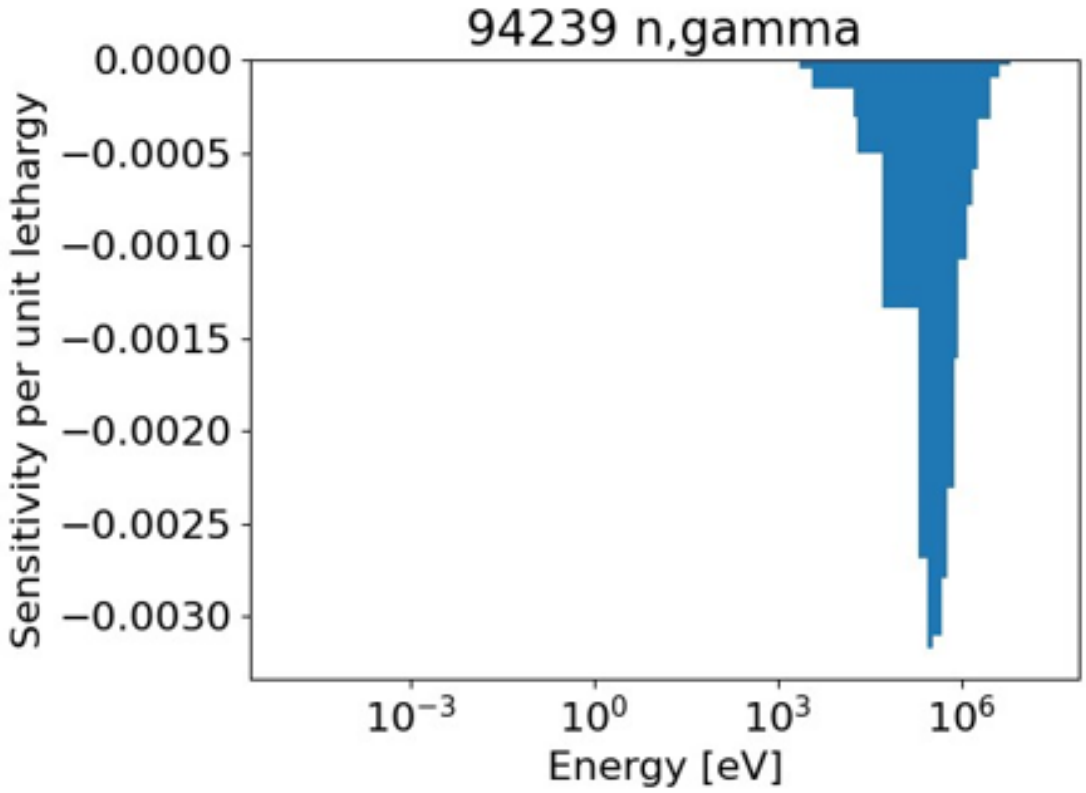

Figure 3.3: This figure shows an example of the visualization of a sensitivity vector normalized per unit lethargy generated with TOFFEE.

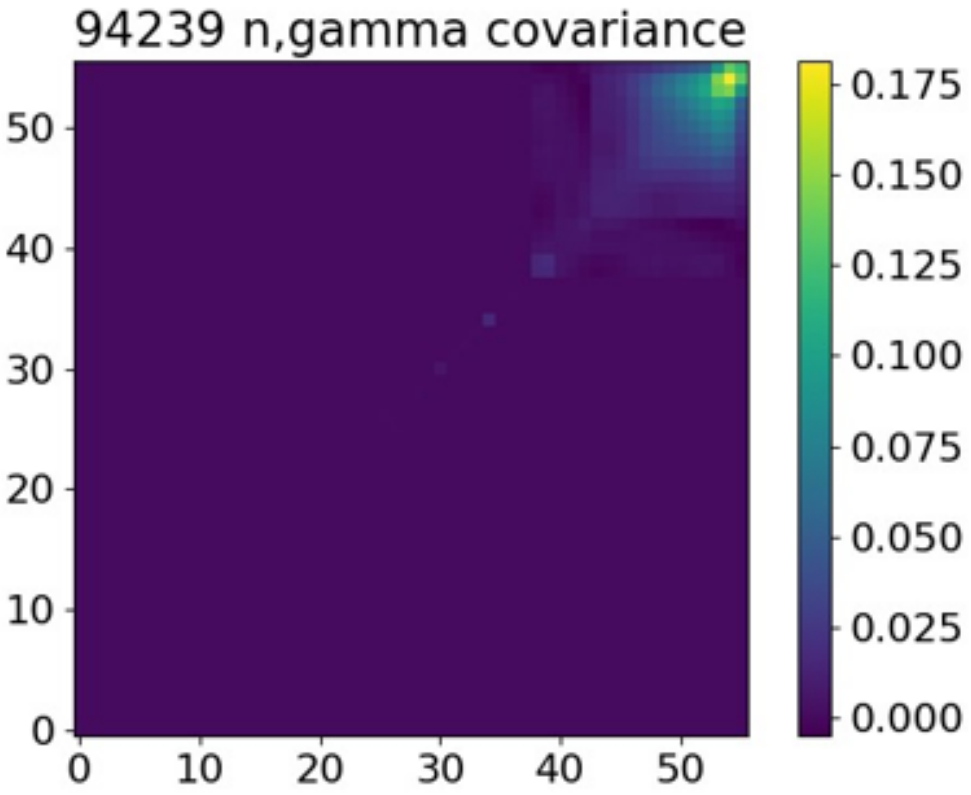

Figure 3.4: This figure shows an example of the visualization of a covariance matrix generated with TOFFEE.

Chapter 4

Applications

4.1 Jezebel Model

Jezebel Favorite (2017b) was a solid sphere of highly enriched plutonium. It was originally constructed to determine the critical mass of plutonium. It was designed to support the early weapons program in the United States. Today, it is still of interest today as a benchmark experiment.

The goal of modeling the Jezebel benchmark in this work is to quantify the uncertainty on the fundamental benchmark. This work also aims to look at the effects of using different cross-section libraries on both k_{eff} and uncertainty. The ENDF VII.1 and ENDF VIII.0 cross-section libraries will be compared for this model. For both libraries, the SCALE 56-group structure was used to construct the covariance matrices and sensitivity vectors. This structure can be seen in the input file for Jezebel in Appendix A.2.

The model used for Jezebel in this work is a solid sphere with a radius of 6.39061 cm. The atom density of the material used is 0.0402901 $\frac{atoms}{barn-cm}$. Table 4.1 shows the nuclide atom densities for the material. The MCNP input can be seen in Appendix A.2.

Table 4.1: This table displays the atom densities used for the material of Jezebel

Nuclide	Atomic Density $[\frac{atoms}{barn-cm}]$
Ga-69	8.2663E-4
Ga-71	5.4857E-4
Pu-239	3.7047E-2
Pu-240	1.7512E-3
Pu-241	1.1674E-4

4.1.1 Results

The k_{eff} of Jezebel was found to be 1.00062 using the ENDF VII.1 library and 1.00056 using the ENDF VIII.0 library. The statistical standard deviation for both cases was 0.00001. The standard deviation of k_{eff} based on the ENDF VII.1 covariance library created using NJOY was found to be 0.00561. The standard deviation using the ENDF VIII.0 covariance library was found to be 0.01004. Both of the calculated k_{eff} values fall well within the error bounds of the experimental value of 1.000 Mosteller et al. (2011) given the respective to the cross-section uncertainty. Table 4.2 shows these results as well as the difference in the calculated and experimental k_{eff}.

One of the interesting results is that the cross-sectional standard deviation grew by a factor of about 1.8. Figure 4.1 and 4.2 shows the top contributors to the cross-sectional uncertainty for the ENDF/B-VII.1 and ENDF/B-VIII.0 library, respectively. It can be seen that the main difference in the uncertainties is the Pu-239 fission cross-section. The sensitivity vectors for both ENDF VII.1 and ENDF VIII.0 visually looked the same as can be seen in Figure 4.3 and 4.4, respectively. However, the covariance matrices are quite different as seen in Figure 4.5 and 4.6, respectively.

The difference in the covariance matrices does seem to account for the difference in the uncertainty between ENDF VII.1 and ENDF VIII.0.

4.2 BeRP Ball

The Beryllium Reflected Plutonium (BeRP) ball was constructed in October of 1980 at Los Alamos Nation Lab Mattingly (2009). It is a sphere of weapons-grade plutonium surrounded by a stainless steel housing. The BeRP ball is one of the subcritical sources that is a part of the National Critical Experiment Research Center (NCERC). It has been used in several recent subcritical and critical benchmark experiments Percher and Kim (2014); Walston et al. (2014).

Table 4.2: This table is a comparison of k_{eff} with different cross-section libraries.

Method	k_{eff}	Statistical STD	Cross-sectional STD	dk
ENDF-VII.1	1.00062	0.00001	0.00561	0.00062
ENDF-VIII.0	1.00056	0.00001	0.01004	0.00056

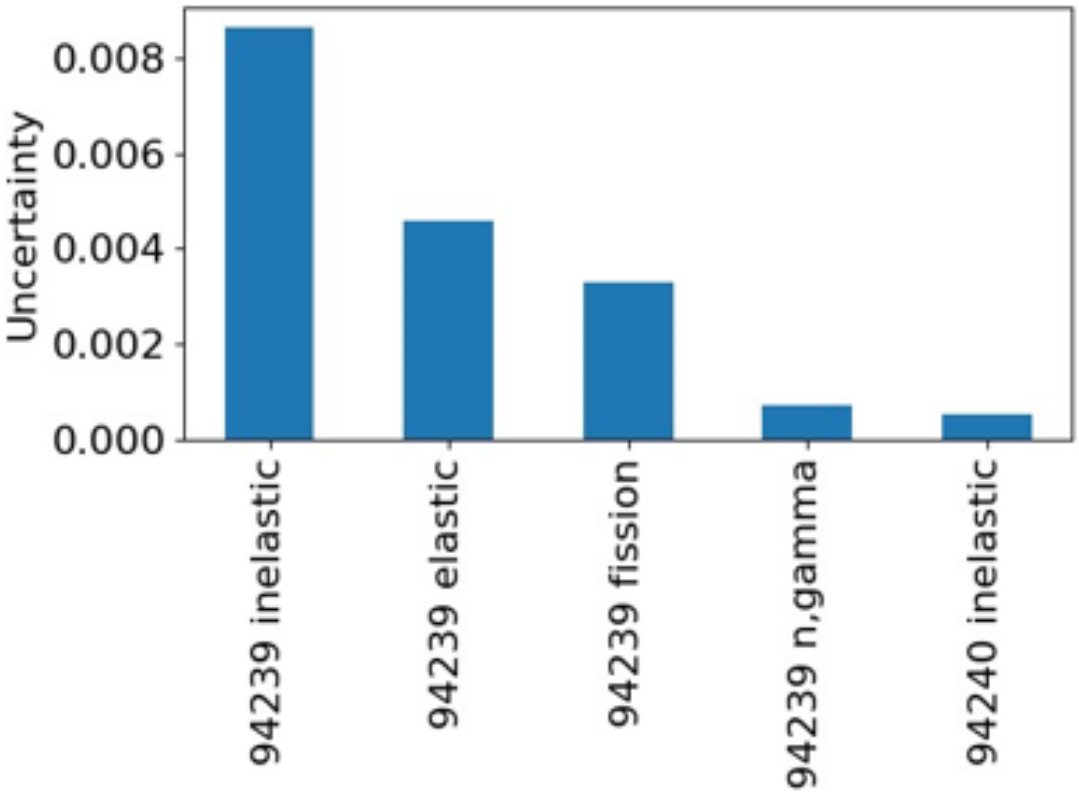

Figure 4.1: This figure shows the top five contributors to the uncertainty for Jezebel using the ENDF/B-VII.1 library.

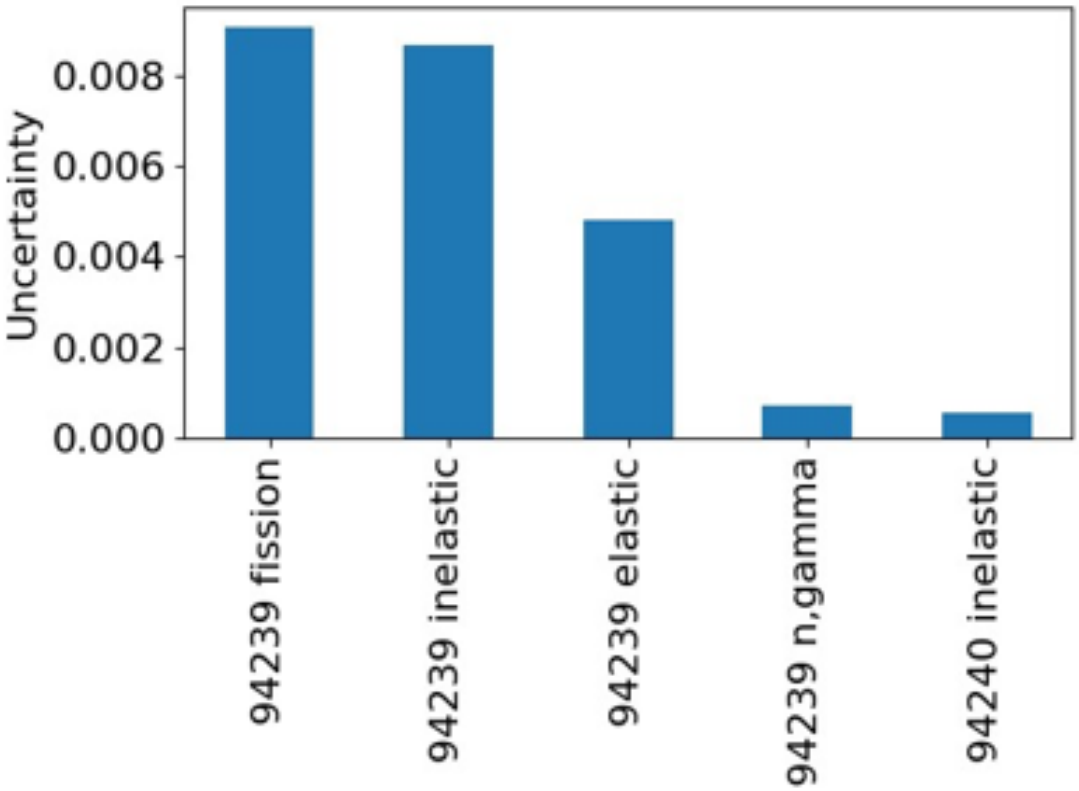

Figure 4.2: This figure shows the top five contributors to the uncertainty for Jezebel using the ENDF/B-VIII.0 library.

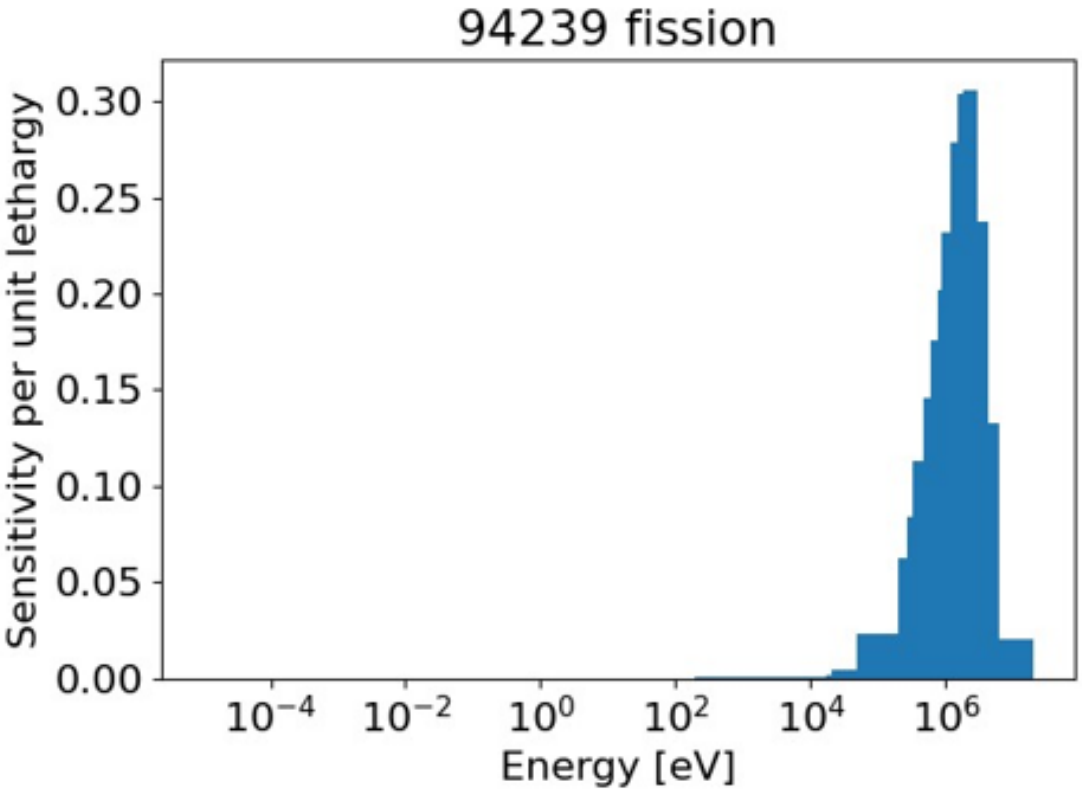

Figure 4.3: This figure shows the sensitivity vector for the Pu-239 fission cross-section. This is for the model of Jezebel using the ENDF/B-VII.1 library.

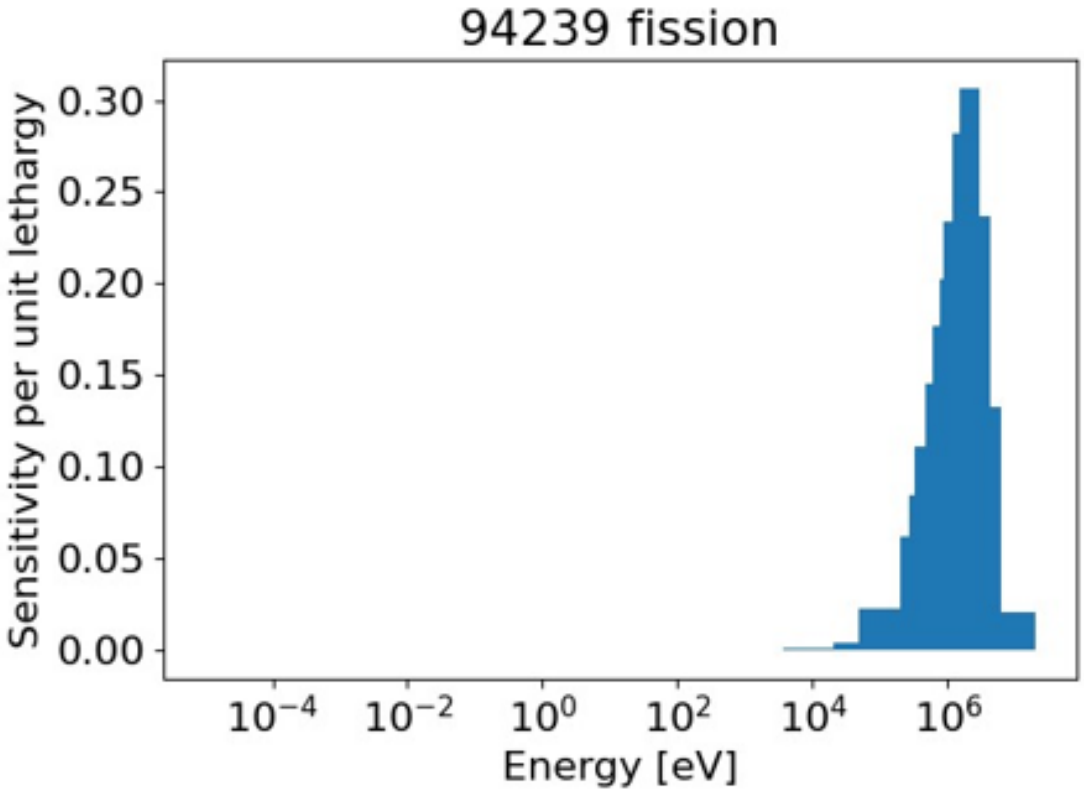

Figure 4.4: This figure shows the sensitivity vector for the Pu-239 fission cross-section. This is for the model of Jezebel using the ENDF/B-VIII.0 library.

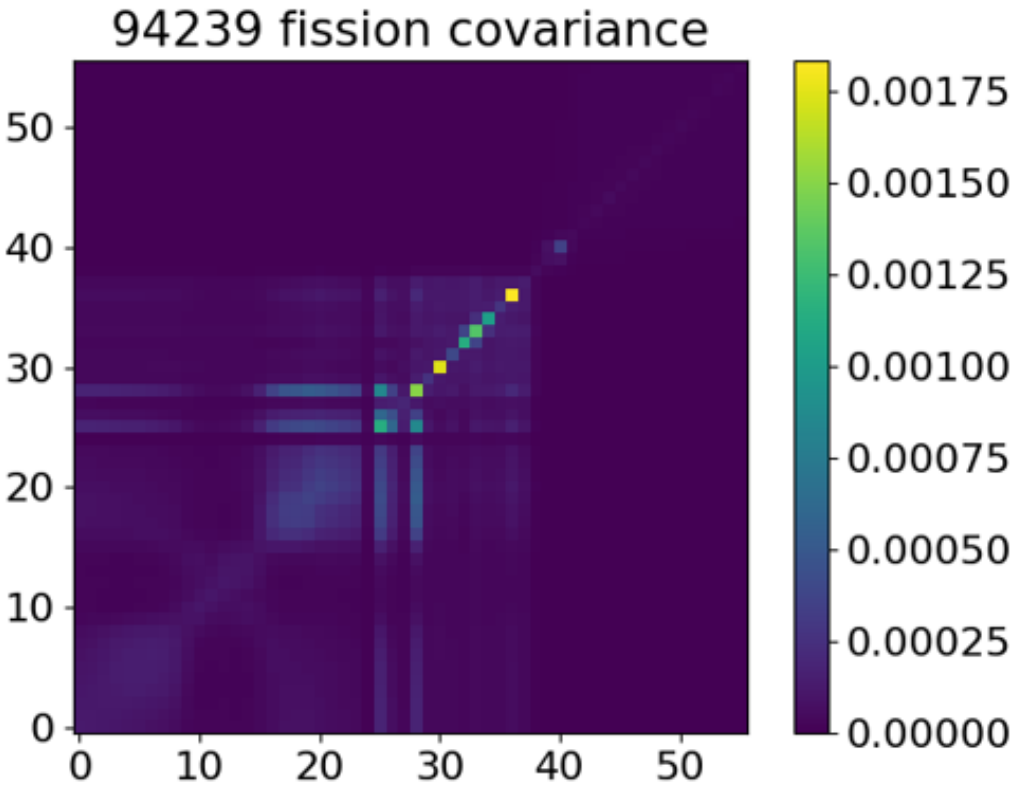

Figure 4.5: This figure shows the covariance matrix for the Pu-239 fission cross-section. This is for the model of Jezebel using the ENDF/B-VII.1 library.

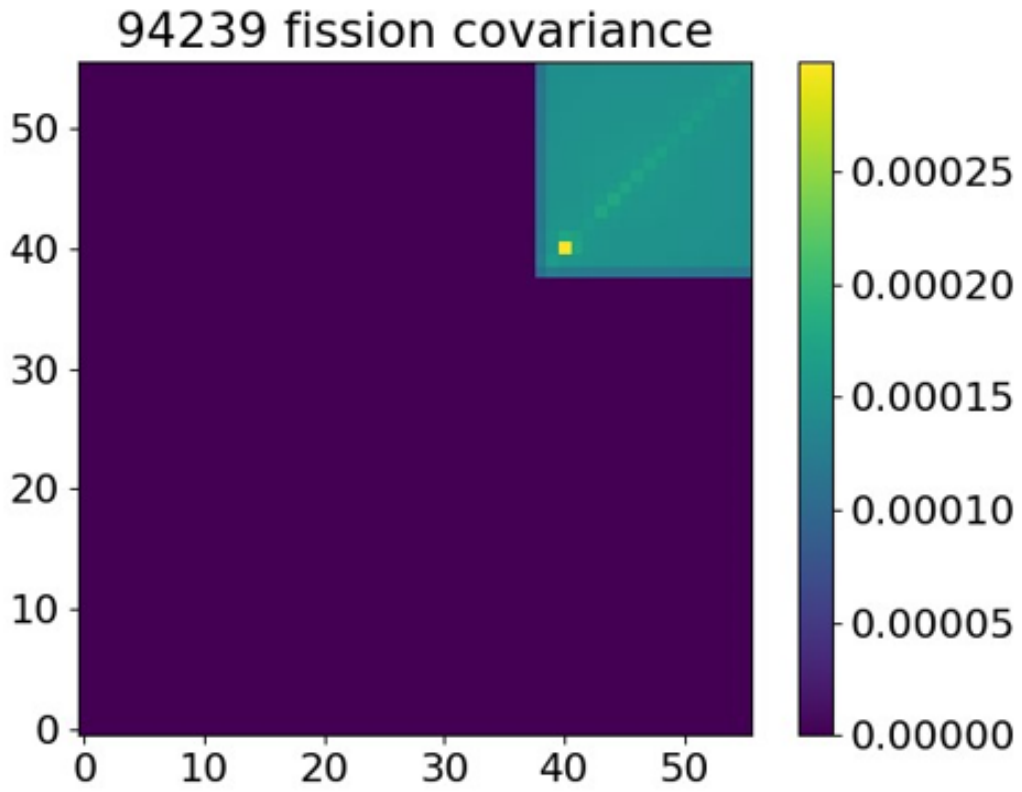

Figure 4.6: This figure shows the covariance matrix for the Pu-239 fission cross-section. This is for the model of Jezebel using the ENDF/B-VIII.0 library.

The BeRP ball is modeled to compare the SCALE Sampler method to calculate uncertainties with the implementation of the MCNP sensitivity method. The k_{eff} and volumetric flux were compared.

4.2.1 Model

The model for BeRP used in this work is a simplified version of the plutonium core. The model is a solid sphere geometry similar to the Jezebel model with a radius of 3.7938 cm. The atom density used is 0.0496932 $\frac{atoms}{barn-cm}$. Table 4.3 shows the atom densities for the model. The ENDF VIII.0 cross-section library was used for both MCNP and SCALE with the 56-group structure used for the covariance and sensitivity vectors.

The SCALE code used is SCALE 6.3. CSAS-VI with KENO-VI is used to calculate k_{eff} with continuous energy cross-sections. Mavric is used to calculate the volumetric flux of the BeRP ball with continuous energy cross-sections. The Sampler module uses both of these codes to calculate the respective cross-section uncertainties. This requires both CSAS-VI and Mavric to be operated in a multigroup mode so the SCALE 252-group structure was used. All of the MCNP and SCALE input files can be seen in Appendix A.3

4.2.2 Results

The experimental value of k_{eff} of BeRP ball is 0.774 Walston et al. (2014). The k_{eff} was found to be 0.77112 using MCNP and 0.77098 using CSAS-VI. The statistical standard deviation was 0.00005 for MCNP and 0.00001 for CSAS-VI. The standard deviation of k_{eff} using the MCNP method was found to be 0.00796. The standard deviation of k_{eff} using the SCALE method was found to be 0.00423. Both of the calculated k_{eff} values fall well within the error bounds of the experimental value given the respective to the cross-section uncertainty. Table 4.4 shows these results as well as the difference in the calculated and experimental k_{eff}.

Table 4.3: This table displays the atom densities used for the material of BeRP ball.

Nuclide	Atomic Density $[\frac{atoms}{barn-cm}]$
C-12	2.2603101e-4
Na-23	1.2836101e-5
Ga-69	3.4079597e-5
Ga-71	2.2623127e-5
Ta-181	1.1596455e-4
W-182	3.0250785e-5
W-183	1.6335000e-5
W-184	3.4969353e-5
W-186	3.2450107e-5
U-235	4.2317089e-5
U-236	9.8159972e-6
Pu-238	7.6626417e-6
Pu-239	4.6016003e-2
Pu-240	2.9011139e-3
Pu-241	2.7811478e-5
Pu-242	1.3585872e-5
Am-241	1.2556189e-4

Table 4.4: This table is a comparison of k_{eff} uncertainty using different methods of calculation.

Method	k_{eff}	Statistical STD	Cross-sectional STD	dk	Run Time
MCNP	0.77119	0.00005	0.00798	0.00281	1160
KENO-VI	0.77077	0.00005	0.00837	0.00323	7590

All flux tallies refer to the volumetric flux per source particle. The flux was found to be 0.0492193 cm^{-2} using MCNP and 0.77098 cm^{-2} using Mavric. The statistical standard deviation was 0.0000836 for MCNP and 0.00001 for Mavric. The standard deviation of the flux using the MCNP method was found to be 0.0006269. The standard deviation of the flux using the SCALE method was found to be 0.00423. Table 4.5 shows the results described above.

4.3 Energy-Tuning Assembly

The last model to test the MCNP Python framework is the energy-tuning assembly designed by the author to tailor 2.5 MeV neutrons generated by a D-D, for AWCC application which is discussed in the motivations section. This model is used as an example of how the framework would support an optimization design driven by cross-section uncertainties propagation for an energy-discretized surface flux out of the ETA.

4.3.1 ETA Model for AWCC

The model used can be seen in Figure 4.7. The ETA consists of a point neutron source with an energy of 2.5 MeV, a 5 cm x 5 cm x 8.784 cm slab of high-density polyethylene (HDPE), and a 1 cm x 1 cm x 1 cm cube of enriched uranium. The materials used for the HDPE and uranium can be seen in Table 4.6 and 4.7. The input file used can be seen in Appendix A.4. The flux is discretized into a 75-group structure as seen in the MCNP input file.

4.3.2 Results

All flux tallies refer to the surface flux per source particle. The total flux was found to be 0.0123694 cm^{-2} using MCNP. The statistical standard deviation was 0.0000557 for MCNP. The standard deviation of the flux using the MCNP method was found

to be 0.0000355. Table 4.8 shows the results described above. Figure 4.8 shows the energy-dependent flux. The left image does contain the cross-sectional despite the values being too small to see. The right image is a zoomed-in look at some of the data points to show the magnitude of the uncertainties.

Table 4.5: This table is a comparison of flux uncertainty calculation methods.

Method	ϕ $[cm^{-2}]$	Statistical STD	Cross-sectional Variance	Run Time
MCNP	0.0491943	0.0000246	0.00180048	1904
Mavric	0.050457	0.000050	0.00186165	2904

Table 4.6: This table displays the atom densities used for the material of high-density polyethylene in the energy-tuning assembly.

Nuclide	Atomic Density $[\frac{atoms}{barn-cm}]$
H-1	0.079855
C-12	0.039929

Table 4.7: This table displays the atom densities used for the material of uranium in the energy-tuning assembly.

Nuclide	Atomic Density $[\frac{atoms}{barn-cm}]$
U-234	0.000013
U-235	0.001456
U-236	0.000007
U-238	0.046468

Table 4.8: This table lists the total flux Out of the energy-tuning assembly.

Model	ϕ	Statistical STD	Cross-sectional Variance
ETA	0.0123694	0.0000557	0.0000355

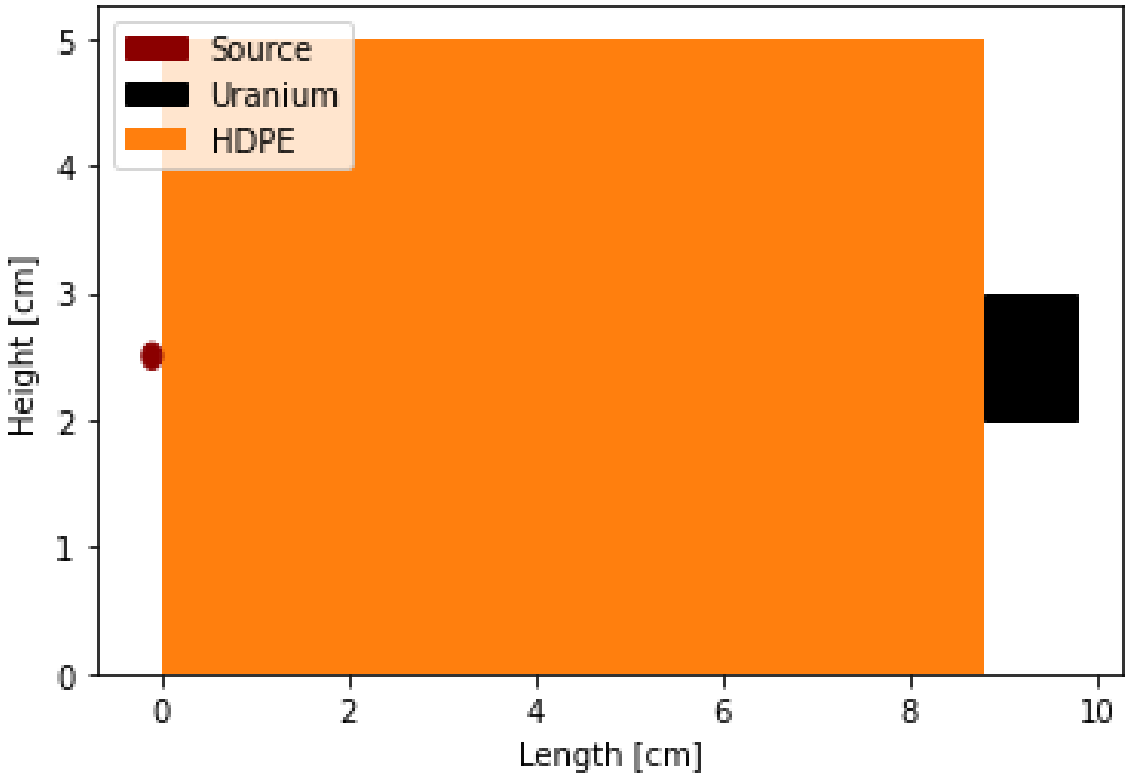

Figure 4.7: This figure shows the design of the energy-tuning assembly designed using Gnowee Williams and Bogetic (2020).

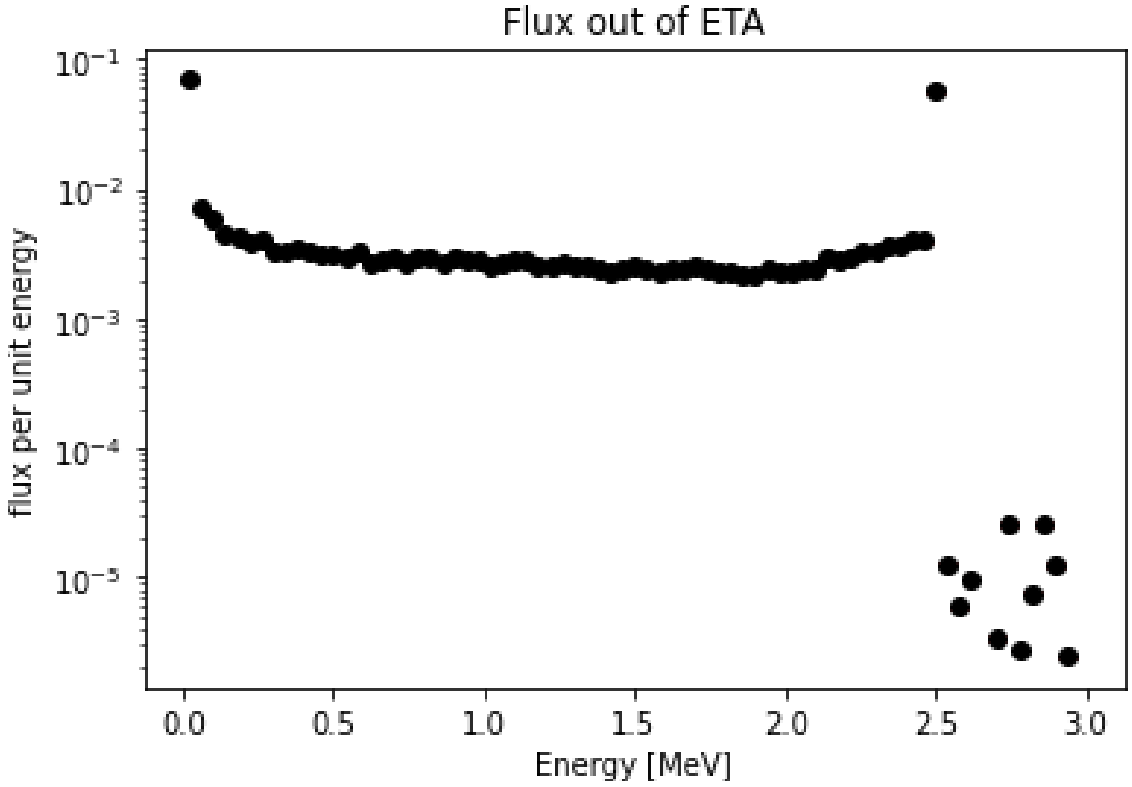

Figure 4.8: This figure shows the surface flux out of the energy-tuning assembly with cross-sectional and statistical error bars.

Chapter 5

Conclusions

This thesis aims to demonstrate the need for an uncertainty analysis tool that can calculate the uncertainty in neutron transport problems for the purpose of optimization. This tool will be useful to both examine the uncertainty in a system during the optimization process and design systems with uncertainty as the driving objective. The goal of this work is to construct a framework, TOFFEE, that uses the capabilities that are present within neutron transport codes, i.e. MCNP-6.3, SCALE, Serpent, etc., to calculate these uncertainties. This framework will be useful for many applications including uncertainty analysis and system design. The approach to designing this framework is to examine the principles of uncertainty propagation for neutron transport. Next, a methodology for the framework is determined to conduct the uncertainty analysis. Then, the framework was demonstrated on several applications that included benchmark experiments and designed experiments.

Uncertainty is incredibly important for describing advanced reactors, subcritical experiments, and radiological source replacement design. These systems are important for the development of many new designs. The uncertainty from nuclear data is one of the key components of the uncertainty for these systems. This work constructs an application that aims to fill this need.

The framework is designed to calculate the cross-section uncertainty on transport problems using the sandwich rule. This method is used to calculate the uncertainty for the Monte Carlo method of neutron transport. The sandwich rule uses a sensitivity vector and covariance matrix for a given cross-section to calculate the uncertainty.

Python is used as the programming language used to construct the framework. MCNP-6.3 is used to calculate the sensitivity vector. NJOY2021 is used to construct the covariance matrix library. The sandwich rule is calculated within the Python framework. The framework is capable of producing valuable information about the uncertainty, sensitivity, and covariance data.

The framework was able to calculate the uncertainty of these experiments despite the difference in the characteristics required. It is capable of calculating the uncertainty in k_{eff} for the historical experiment Jezebel. The calculated k_{eff} value using MCNP6.3 was 1.00058 with a cross-sectional standard deviation of 0.01004.

The framework calculated the uncertainty in both k_{eff} and flux for the BeRP ball subcritical benchmark experiment. The calculated k_{eff} value using MCNP6.3 was 0.77119 with a cross-sectional standard deviation of 0.00798. The calculated volumetric flux value using MCNP6.3 was 0.0491943 $cm^{-}2$ with a cross-sectional standard deviation of 0.00180048.

The framework is also capable of calculating the cross-section uncertainty in the energy-dependent flux out of a designed ETA for source replacement. The calculated energy-integrated surface flux value using MCNP6.3 was 0.0134694 $cm^{-}1$ with a cross-sectional standard deviation of 0.0000355.

In conclusion, a Python framework was created to automate the process of generating a covariance library for a specific energy group structure and conduct a sensitivity analysis using MCNP6.3 for the purpose of conducting uncertainty analysis. The framework was capable of producing uncertainty in all of the required quantities of interest. The framework compared well to the alternative method in regard to optimization. For this reason, it is believed that the Python framework

constructed in this work is a suitable method to calculate cross-section uncertainties for the purpose of system optimization.

Bibliography

Agency, N. E. (2023). Icsbep handbook 2021. 18

Bevins, J. E. and Slaybaugh, R. N. (2019). Gnowee: a hybrid metaheuristic optimization algorithm for constrained, black box, combinatorial mixed-integer design. *Nuclear Technology*, 205(4):542–562. 2

Bogetic, S., Bevins, J. E., Bernstein, L. A., Slaybaugh, R., and Vujic, J. (2018). Metaheuristic optimization method for neutron spectra shaping. 2

Brown, D. A., Chadwick, M., Capote, R., Kahler, A., Trkov, A., Herman, M., Sonzogni, A., Danon, Y., Carlson, A., Dunn, M., et al. (2018). Endf/b-viii. 0: the 8th major release of the nuclear reaction data library with cielo-project cross sections, new standards and thermal scattering data. *Nuclear Data Sheets*, 148:1–142. 12

BUC, D. and MASÁROVÁ, G. (2013). Application of monte carlo simulation in the field of mechanical engineering. *Ad Alta: Journal of Interdisciplinary Research*, 3(2). 17

Chowdhury, S., Camsari, K. Y., and Datta, S. (2023). Accelerated quantum monte carlo with probabilistic computers. *Communications Physics*, 6(1):85. 17

Conant, A., Nelson, N., Navarro, J., Grimm, T., Denbrock, C., and Wahlen, R. (2023). Mcnp neutronic design optimization of an accelerator-driven subcritical

assembly for mo-99 production. Technical report, Oak Ridge National Laboratory (ORNL), Oak Ridge, TN (United States). 1

Davison, B. (1957). *Neutron Transport Theory*. International series of monographs on physics. Clarendon Press. 7

De Gregorio, A. G. (2005). Neutron physics in the early 1930s. *Historical studies in the physical and biological sciences*, 35(2):293–340. 1

Depriest, K., Miller, J., and Henderson, S. (2022). Updates to snl nuclear criticality safety benchmark suite for mcnp. Technical report, Sandia National Lab.(SNL-NM), Albuquerque, NM (United States). 1

Favorite, J. (2017a). Using the mcnp taylor series perturbation feature (efficiently) for shielding problems. In *EPJ Web of Conferences*, volume 153, page 06030. EDP Sciences. 21

Favorite, J. A. (2017b). Jezebel: reconstructing a critical experiment from 60 years ago. Technical report, Los Alamos National Lab.(LANL), Los Alamos, NM (United States). 17, 30

Favorite, J. A. (2021). (u) using the mcnp6 perturbation capability for source nuclide density sensitivities. Technical report, Los Alamos National Lab.(LANL), Los Alamos, NM (United States). 21

Fleming, M., Chadwick, M., Brown, D., Capote, R., Ge, Z., Herman, M., Ignatyuk, A., Ivanova, T., Iwamoto, O., Koning, A., et al. (2020). Results of the collaborative international evaluated library organisation (cielo) project. In *EPJ Web of Conferences*, volume 239. EDP Sciences. 15

Glasserman, P. (2004). *Monte Carlo methods in financial engineering*, volume 53. Springer. 17

Hahn, O. and Strassmann, F. (1938). Die chemische abscheidung der bei der spaltung des uran. *Naturwissenschaften*, 26:756. 1

Hines, W., Pevey, J., and Sobes, V. (2018). Preliminary design of a fast flux user facility at the university of tennessee. Technical report, Oak Ridge National Lab.(ORNL), Oak Ridge, TN (United States). 4

Kahler III, A. and Macfarlane, R. (2016). Njoy2016. Technical report, Los Alamos National Lab.(LANL), Los Alamos, NM (United States). 23

Kiedrowski, B. C. (2013). Mcnp6. 1 k-eigenvalue sensitivity capability: a user's guide. Technical report, Los Alamos National Lab.(LANL), Los Alamos, NM (United States). 20

Kiedrowski, B. C., Brown, F. B., Conlin, J. L., Favorite, J. A., Kahler, A. C., Kersting, A. R., Parsons, D. K., and Walker, J. L. (2015). Whisper: Sensitivity/uncertainty-based computational methods and software for determining baseline upper subcritical limits. *Nuclear Science and Engineering*, 181(1):17–47. 16

Kulesza, J. A., Adams, T. R., Armstrong, J. C., Bolding, S. R., Brown, F. B., Bull, J. S., Burke, T. P., Clark, A. R., Forster III, R. A. A., Giron, J. F., et al. (2022). Mcnp® code version 6.3. 0 theory & user manual. Technical report, Los Alamos National Lab.(LANL), Los Alamos, NM (United States). 19, 21

Leppänen, J., Pusa, M., Viitanen, T., Valtavirta, V., and Kaltiaisenaho, T. (2015). The serpent monte carlo code: Status, development and applications in 2013. *Annals of Nuclear Energy*, 82:142–150. 20

Lewis, E. E. and Miller, W. F. (1984). Computational methods of neutron transport. 8

Little, R., Kawano, T., Hale, G., Pigni, M., Herman, M., Obložinskỳ, P., Williams, M., Dunn, M., Arbanas, G., Wiarda, D., et al. (2008). Low-fidelity covariance project. *Nuclear Data Sheets*, 109(12):2828–2833. 15

Mattingly, J. K. (2009). Polyethylene-reflected plutonium metal sphere: subcritical neutron and gamma measurements. Technical report, Sandia National Laboratories (SNL), Albuquerque, NM, and Livermore, CA 32

McElroy, R. D. and Cleveland, S. L. (2017). The dd neutron generator as an alternative to am (li) isotopic neutron source in the uranium neutron coincidence collar. Technical report, Oak Ridge National Lab.(ORNL), Oak Ridge, TN (United States). 2

McElroy, R. D. and Cleveland, S. L. (2018). The dd neutron generator as an alternative to the am (li) isotopic neutron source in active neutron coincidence counting for international nuclear safeguards. Technical report, Oak Ridge National Lab.(ORNL), Oak Ridge, TN (United States). 2

Metropolis, N., Bivins, R., Storm, M., Miller, J., Friedlander, G., and Turkevich, A. (1958). Monte carlo calculations on intranuclear cascades. ii. high-energy studies and pion processes. *Physical Review*, 110(1):204. 17, 20

Mosteller, R. D., Brown, F. B., and Kiedrowski, B. C. (2011). An expanded criticality validation suite for mcnp. *Transactions of the American Nuclear Society*, 104:453. 32

Percher, C. and Kim, S. (2014). Llnl preliminary design for the berp ball with composite polyethylene and nickel reflection. Technical report, Lawrence Livermore National Lab.(LLNL), Livermore, CA (United States). 32

Pevey, J., Chvála, O., Davis, S., Sobes, V., and Hines, J. W. (2020). Genetic algorithm design of a coupled fast and thermal subcritical assembly. *Nuclear Technology*, 206(4):609–619. x, 4, 6

Pevey, J., Sobes, V., and Hines, W. J. (2022). Neural network acceleration of genetic algorithms for the optimization of a coupled fast/thermal nuclear experiment. *Frontiers in Energy Research*, 10:874194. 4

Plompen, A. J., Cabellos, O., De Saint Jean, C., Fleming, M., Algora, A., Angelone, M., Archier, P., Bauge, E., Bersillon, O., Blokhin, A., et al. (2020). The joint evaluated fission and fusion nuclear data library, jeff-3.3. *The European Physical Journal A*, 56(7):1–108. 12

Quartemont, N. J., Peterson, G., Moran, C., Samin, A., Wang, B., Yeamans, C., Woodworth, B., Holland, D., Petrosky, J. C., and Bevins, J. E. (2021). Athena: A unique radiation environment platform at the national ignition facility. *Nuclear Instruments and Methods in Physics Research Section A: Accelerators, Spectrometers, Detectors and Associated Equipment*, 1016:165777. x, 2, 3

Rising, M. E. and Bolding, S. R. (2022). Coincident capture through post-processing ptrac. Technical report, Los Alamos National Lab.(LANL), Los Alamos, NM (United States). 1

Romano, P. K., Horelik, N. E., Herman, B. R., Nelson, A. G., Forget, B., and Smith, K. (2015). Openmc: A state-of-the-art monte carlo code for research and development. *Annals of Nuclear Energy*, 82:90–97. 19

Shaw, A., Bostelmann, R., Hartanto, D., Walker, E., and Wieselquist, W. (2023). Scale modeling of the sodium cooled fast-spectrum advanced burner test reactor. Technical report, Oak Ridge National Laboratory (ORNL), Oak Ridge, TN (United States). 1, 17

Sobes, V., Pevey, J., Depillis, A., Chvala, O., Bogetic, S., and Hines, W. (2022). The fast neutron source at utk: a project with massimo salvatores. In *Proceedings of the international conference on physics of reactors-PHYSOR 2022*. 4

Variansyah, I., Morgan, J., Northrop, J., Niemeyer, K. E., and McClarren, R. G. (2023). Development of mc/dc: a performant, scalable, and portable python-based monte carlo neutron transport code. *arXiv preprint arXiv:2305.07636*. 1

Walston, S., Burch, J., Cowan, M., Guethlein, G., Keefer, G., Kerr, P., McAvoy, D., Nakae, L., Prasad, M., Pugh, D., et al. (2014). Benchmark measurements of the berp ball in various reflectors. Technical report, Lawrence Livermore National Lab.(LLNL), Livermore, CA (United States). 32, 40

Wiarda, D., Williams, M. L., Celik, C., and Dunn, M. E. (2015). Ampx: A modern cross section processing system for generating nuclear data libraries. Technical report, Oak Ridge National Lab.(ORNL), Oak Ridge, TN (United States). 23

Wieselquist, W. A. and Lefebvre, R. A. (2021). Scale 6.3. 0 user manual. Technical report, Oak Ridge National Laboratory (ORNL), Oak Ridge, TN (United States). 19

Wigner, E. P. and Breit, G. (1992). *Approximation for Radius of Sphere Sufficient for Chain Reaction in Light Isotope*, pages 142–148. Springer Berlin Heidelberg, Berlin, Heidelberg. 1

Williams, A. and Bogetic, S. (2020). Metaheuristics design of an energy tuning assembly to replace amli source within active well coincidence counter (awcc). In *ANS Winter Meeting*. xi, 2, 46

Winch, N. M., Madden, A. C., Hunter, J. F., Ronald, O., et al. (2017). Detector performance for fast neutron radiography and computed tomography. In *2017 IEEE Nuclear Science Symposium and Medical Imaging Conference (NSS/MIC)*, pages 1–6. IEEE. 2

Yinghuai, Z. and Hosmane, N. S. (2013). Applications and perspectives of boron-enriched nanocomposites in cancer therapy. *Future medicinal chemistry*, 5(6):705–714. 2

Appendix

Appendix A

Input Files

A.1 NJOY Input File

```
moder
  20 -30 /
reconr
  -30 -31 /
  'automated processing using ndvv.njoy.process see *.log files' /
  %%isotope_endf_value%% 0 0 /
  0.001 0.0 0.01 5.0000000000000004e-08 /
  0 /
broadr
  -30 -31 -32 /
  %%isotope_endf_value%% 1 0 0 0.0 /
  0.001 1000000.0 0.01 5.0000000000000004e-08 /
  293.6
  0 /
heatr
  -30 -32 -33 /
```

```
  %%isotope_endf_value%% 3 0 0 0 2 /
  442
  443
  444
gaspr
  -30 -33 -34 /
thermr
  0 -34 -35 /
  0 %%isotope_endf_value%% 16 1 1 0 0 1 221 2 /
  293.6 /
  0.001 10.0 /
moder
  -35 21/
errorr
20 21 0 33/
%%isotope_endf_value%% 1 9 0 1/
0 293.6 /
0 33 0/
%%energy_bins_length%%/
%%energy_bins%%/
stop
```

A.2 Jezebel Input File

```
Pu239 Jezebel 17,065.5 g Pu-alloy (4.5 at% 240Pu, 1.02 wt% Ga)
1  94   0.0402901     -1    imp:n=1
2   0                  1    imp:n=0

1    so     6.39061
```

```
mode     n
rand gen=2 seed=2901000001
prdmp j 500
kcode 2400000 1.0 50 1050
totnu
sdef pos=0. 0. 0. rad=d1 erg=d2
si1 0.  6.39061
sp1 -21 2
sp2  -3  0.966  2.842
c Materials
m94   94239.00c 3.7047E-02
      94240.00c 1.7512E-03
      94241.00c 1.1674E-04
      31069.00c 8.2663E-04
      31071.00c 5.4857E-04
c End Materials
print
c Pu239 Jezebel 17,065.5 g Pu-al
```

A.3 Berp Input Files

A.3.1 k_{eff}

```
very simplified MCNP input deck for FUND-NCERC-PU-HE3-MULT-001-001 to compute a multigroup weighting spectrum.
c cell cards.
100 100 4.96932E-02     -100    imp:n=1 $ BeRP ball.
970 0                   +100    -999    imp:n=1 $ void between assembly and problem boundary.
999 0                   +999            imp:n=0 $ outside of problem.
```

```
c surface cards.
100 so  3.79380000e+00  $ BeRP ball.
999 so  1.50000000e+01  $ problem boundary.

c
kcode 100000 1.0 100 1100
sdef    pos=0.  0.  0.
        rad=d1
        erg=d2
si1 0 3.79380000e+00
sp1 -21 2
si2 h   1.00000000000000E-11 2.96937332818714E-09 1.03641312841130E-08
        2.99896082485731E-08 4.09909343950883E-08 4.94445050193864E-08
        7.19413303032538E-08 1.04674017947447E-07 1.52000000000000E-07
        2.21594897733660E-07 2.51099915574398E-07 2.84533480898340E-07
        3.22418673725673E-07 3.65348221372105E-07 4.14000000000000E-07
        6.41206097331274E-07 1.13000000000000E-06 3.06000000000000E-06
        8.32000000000000E-06 2.26000000000000E-05 6.14000000000000E-05
        1.67000000000000E-04 4.54000000000000E-04 1.23500000000000E-03
        3.35000000000000E-03 9.12000000000000E-03 2.48000000000000E-02
        6.76000000000000E-02 1.84000000000000E-01 3.03000000000000E-01
        5.00000000000000E-01 8.23000000000000E-01 1.35300000000000E+00
        1.73800000000000E+00 2.23200000000000E+00 2.86500000000000E+00
        3.68000000000000E+00 4.72366552741015E+00 5.35261428518990E+00
        6.07000000000000E+00 6.87289278790972E+00 7.79000000000000E+00
        8.82496902584595E+00 1.00000000000000E+01 1.20000000000000E+01
        1.30000000000000E+01 1.35000000000000E+01 1.40000000000000E+01
        1.45000000000000E+01 1.50000000000000E+01 1.70000000000000E+01
        2.00000000000000E+01
sp2 d   0.00000000E+00 8.18650845E-11 4.51194069E-10 2.09066962E-09
        1.56889389E-09 1.36178437E-09 4.19327253E-09 7.36071819E-09 1.28283369E-08
        2.27598005E-08 1.08686190E-08 1.31069010E-08 1.58150423E-08 1.90689469E-08
        2.30150300E-08 1.24810990E-07 3.47438649E-07 2.09727143E-06 9.41892725E-06
```

```
        4.21673904E-05 1.89017851E-04 8.49590673E-04 3.80522161E-03 1.71016048E-02
        7.62671485E-02 3.42367277E-01 1.52632930E+00 6.78053373E+00 2.92631491E+01
        3.95363440E+01 7.71372524E+01 1.39677576E+02 2.24058616E+02 1.41941658E+02
        1.50161138E+02 1.42728970E+02 1.18479736E+02 8.15821435E+01 2.62680554E+01
        1.75890211E+01 1.07715140E+01 5.80464169E+00 2.80739188E+00 1.19672667E+00
        5.23540941E-01 5.78899514E-02 1.35298252E-02 8.63996102E-03 5.26677206E-03
        3.16021557E-03 4.41688552E-03 6.69524739E-04
c
c materials cards.
c
c BeRP ball.
c Materials
m100    6012.00c  2.2603101e-4
        11023.00c 1.2836101e-5
        31069.00c 3.4079597e-5
        31071.00c 2.2623127e-5
        73181.00c 1.1596455e-4
        74182.00c 3.0250785e-5
        74183.00c 1.6335000e-5
        74184.00c 3.4969353e-5
        74186.00c 3.2450107e-5
        92235.00c 4.2317089e-5
        92236.00c 9.8159972e-6
        94238.00c 7.6626417e-6
        94239.00c 4.6016003e-2
        94240.00c 2.9011139e-3
        94241.00c 2.7811478e-5
        94242.00c 1.3585872e-5
        95241.00c 1.2556189e-4
c End Materials
```

A.3.2 Flux

```
very simplified MCNP input deck for FUND-NCERC-PU-HE3-MULT-001-001 to compute a multigroup weighting spectrum.
c cell cards.
100 100 4.96932E-02     -100    imp:n=1 $ BeRP ball.
970 0                   +100    -999    imp:n=1 $ void between assembly and problem boundary.
999 0                   +999            imp:n=0 $ outside of problem.

c surface cards.
100 so  3.79380000e+00  $ BeRP ball.
999 so  1.50000000e+01  $ problem boundary.

c data cards.
print   10  40  85  110
c
c general source distribution.
c
nps 3e+07
c prdmp  j 500000 -1 2 $ how often to dump to the run tape and write a MCTAL file.
sdef    pos=0.  0.  0.
        rad=d1
        erg=d2
c
c spatial distribution.
c
si1 0 3.79380000e+00
sp1 -21 2
c
c energy distribution. source definition in neutrons / sec from SENSMG.
c the normalized number of neutrons emitted in each energy group gives
c the energy distribution.
c region     1 mat     1
c total source in neuts/s:  2.7867023E+05
c         0.00000000E+00 8.18650845E-11 4.51194068E-10 2.09066962E-09
```

```
c         1.56889389E-09 1.36178437E-09 4.19327252E-09 7.36071819E-09 1.28283369E-08
c         2.27598005E-08 1.08686190E-08 1.31069010E-08 1.58150423E-08 1.90689469E-08
c         2.30150300E-08 1.24810990E-07 3.47438649E-07 2.09727142E-06 9.41892724E-06
c         4.21673904E-05 1.89017850E-04 8.49590672E-04 3.80522160E-03 1.71016048E-02
c         7.62671483E-02 3.42367276E-01 1.52632930E+00 6.78053372E+00 2.92631489E+01
c         3.95363439E+01 7.71372523E+01 1.39677575E+02 2.24058615E+02 1.41941658E+02
c         1.50161138E+02 1.42728970E+02 1.18479736E+02 8.15821434E+01 2.62680552E+01
c         1.75890209E+01 1.07715139E+01 5.80464166E+00 2.80739187E+00 1.19672667E+00
c         5.23540941E-01 5.78899513E-02 1.35298252E-02 8.63996101E-03 5.26677205E-03
c         3.16021557E-03 4.41688551E-03 6.69524738E-04
c
si2 h   1.00000000000000E-11 2.96937332818714E-09 1.03641312841130E-08
        2.99896082485731E-08 4.09909343950883E-08 4.94445050193864E-08
        7.19413303032538E-08 1.04674017947447E-07 1.52000000000000E-07
        2.21594897733660E-07 2.51099915574398E-07 2.84533480898340E-07
        3.22418673725673E-07 3.65348221372105E-07 4.14000000000000E-07
        6.41206097331274E-07 1.13000000000000E-06 3.06000000000000E-06
        8.32000000000000E-06 2.26000000000000E-05 6.14000000000000E-05
        1.67000000000000E-04 4.54000000000000E-04 1.23500000000000E-03
        3.35000000000000E-03 9.12000000000000E-03 2.48000000000000E-02
        6.76000000000000E-02 1.84000000000000E-01 3.03000000000000E-01
        5.00000000000000E-01 8.23000000000000E-01 1.35300000000000E+00
        1.73800000000000E+00 2.23200000000000E+00 2.86500000000000E+00
        3.68000000000000E+00 4.72366552741015E+00 5.35261428518990E+00
        6.07000000000000E+00 6.87289278790972E+00 7.79000000000000E+00
        8.82496902584595E+00 1.00000000000000E+01 1.20000000000000E+01
        1.30000000000000E+01 1.35000000000000E+01 1.40000000000000E+01
        1.45000000000000E+01 1.50000000000000E+01 1.70000000000000E+01
        2.00000000000000E+01
sp2 d   0.00000000E+00 8.18650845E-11 4.51194069E-10 2.09066962E-09
        1.56889389E-09 1.36178437E-09 4.19327253E-09 7.36071819E-09 1.28283369E-08
        2.27598005E-08 1.08686190E-08 1.31069010E-08 1.58150423E-08 1.90689469E-08
        2.30150300E-08 1.24810990E-07 3.47438649E-07 2.09727143E-06 9.41892725E-06
        4.21673904E-05 1.89017851E-04 8.49590673E-04 3.80522161E-03 1.71016048E-02
```

```
        7.62671485E-02 3.42367277E-01 1.52632930E+00 6.78053373E+00 2.92631491E+01
        3.95363440E+01 7.71372524E+01 1.39677576E+02 2.24058616E+02 1.41941658E+02
        1.50161138E+02 1.42728970E+02 1.18479736E+02 8.15821435E+01 2.62680554E+01
        1.75890211E+01 1.07715140E+01 5.80464169E+00 2.80739188E+00 1.19672667E+00
        5.23540941E-01 5.78899514E-02 1.35298252E-02 8.63996102E-03 5.26677206E-03
        3.16021557E-03 4.41688552E-03 6.69524739E-04
c
c materials cards.
c
c BeRP ball.
c Materials
m100    6012.00c  2.2603101e-4
        11023.00c 1.2836101e-5
        31069.00c 3.4079597e-5
        31071.00c 2.2623127e-5
        73181.00c 1.1596455e-4
        74182.00c 3.0250785e-5
        74183.00c 1.6335000e-5
        74184.00c 3.4969353e-5
        74186.00c 3.2450107e-5
        92235.00c 4.2317089e-5
        92236.00c 9.8159972e-6
        94238.00c 7.6626417e-6
        94239.00c 4.6016003e-2
        94240.00c 2.9011139e-3
        94241.00c 2.7811478e-5
        94242.00c 1.3585872e-5
        95241.00c 1.2556189e-4
c End Materials
f4:n 100
```

A.4 Energy Tuning Assembly Input File

```
AmLi source shaping
C
C
C
C ######################## BLOCK 1 ##############################
C
C ###### CELLS ######
1  2008 0.119784 1 -2 3 -4 5 -6 IMP:N=1
2  2008 0.119784 1 -2 3 -4 6 -7 IMP:N=1
3  2008 0.119784 1 -2 3 -4 7 -8 IMP:N=1
4  2008 0.119784 1 -2 3 -4 8 -9 IMP:N=1
5  2008 0.119784 1 -2 3 -4 9 -10 IMP:N=1
6  2008 0.119784 1 -2 3 -4 10 -11 IMP:N=1
7  2008 0.119784 1 -2 3 -4 11 -12 IMP:N=1
8  2008 0.119784 1 -2 3 -4 12 -13 IMP:N=1
9  2008 0.119784 1 -2 3 -4 13 -14 IMP:N=1
10 2008 0.119784 1 -2 3 -4 14 -15 IMP:N=1
11 4000 0.047944 15 -16 17 -18 19 -20 IMP:N=1
100 0 -99 #1 #2 #3 #4 # 5 #6 #7 #8 #9 #10 #11 IMP:N=1
101 0 99 IMP:N=0

C
C
C ######################## BLOCK 2 ##############################
C
C ###### SURFACES ######
1  py -2.5
```

```
2  py 2.5
3  pz -2.5
4  pz 2.5
5  px 0
6  px 0.99999874
7  px 1.6238801999999999
8  px 2.56195476
9  px 3.3975858899999998
10 px 4.1827926
11 px 5.1743757200000005
12 px 6.16882774
13 px 7.15377788
14 px 7.92431155
15 px 8.78376786
16 px 9.78376786
17 py -0.5
18 py 0.5
19 pz -0.5
20 pz 0.5
99 SO 108.78376786 $outer sphere

C
C
C ######################## BLOCK 3 ##############################
C
C ###### MODE ######
MODE N
C
C
```

```
C ###### SOURCE ######
C
sdef par=n erg=2.5 pos=0.000001 0.0 0.0
C
C ###### TALLIES ######
C
F2:N 15
SD2 1.0
E2    0.04
      0.08
      0.12
      0.16
      0.2
      0.24
      0.28
      0.32
      0.36
      0.4
      0.44
      0.48
      0.52
      0.56
      0.6
      0.64
      0.68
      0.72
      0.76
      0.8
      0.84
```

```
0.88
0.92
0.96
1.0
1.04
1.08
1.12
1.16
1.2
1.24
1.28
1.32
1.36
1.4
1.44
1.48
1.52
1.56
1.6
1.64
1.68
1.72
1.76
1.8
1.84
1.88
1.92
1.96
2.0
```

```
      2.04
      2.08
      2.12
      2.16
      2.2
      2.24
      2.28
      2.32
      2.36
      2.4
      2.44
      2.48
      2.52
      2.56
      2.6
      2.64
      2.68
      2.72
      2.76
      2.8
      2.84
      2.88
      2.92
      2.96
      3.0
C
C ###### MATERIALS ######
C
C
```

```
C ###### HISTORY LIMIT ######
C
C
C
C ###### RUN TIME ######
C
nps 10000000
C
print
C
C ######################## ENDING ##############################
c Materials
c Uranium
m4000 92234.00c 0.000013
      92235.00c 0.001456
      92236.00c 0.000007
      92238.00c 0.046468
c Poly (non-borated)
m2008 1001.00c 0.079855
      6012.00c 0.039929
c End Materials
```

Vita

Austin Williams is from Tazewell, TN. He attended Claiborne High School. Austin played varsity football and baseball in high school. Austin began his studies in Nuclear Engineering at the University of Tennessee, Knoxville in 2017. Once he graduated, Austin began his Master's degree work under Dr. Sandra Bogetic. Upon graduation, Austin plans to continue his education to acquire a PhD in nuclear Engineering.